2006-09-07

Design and Fabrication of Rotationally Tristable Compliant Mechanisms

Tyler M. Pendleton
Brigham Young University - Provo

DESIGN AND FABRICATION OF ROTATIONALLY TRISTABLE COMPLIANT MECHANISMS

by

Tyler Max Pendleton

A thesis submitted to the faculty of

Brigham Young University

in partial fulfillment of the requirements for the degree of

Master of Science

Department of Mechanical Engineering

Brigham Young University

Thesis Completed
December 2006

BRIGHAM YOUNG UNIVERSITY

GRADUATE COMMITTEE APPROVAL

of a thesis submitted by

Tyler Max Pendleton

This thesis has been read by each member of the following graduate committee and by majority vote has been found to be satisfactory.

Date	Brian D. Jensen, Chair
Date	Larry L. Howell
Date	Spencer P. Magleby

BRIGHAM YOUNG UNIVERSITY

As chair of the candidate's graduate committee, I have read the thesis of Tyler Max Pendleton in its final form and have found that (1) its format, citations, and bibliographical style are consistent and acceptable and fulfill university and department style requirements; (2) its illustrative materials including figures, tables, and charts are in place; and (3) the final manuscript is satisfactory to the graduate committee and is ready for submission to the university library.

Date

Brian D. Jensen
Chair, Graduate Committee

Accepted for the Department

Matthew R. Jones
Graduate Coordinator

Accepted for the College

Alan R. Parkinson
Dean, Ira A. Fulton College of
Engineering and Technology

ABSTRACT

DESIGN AND FABRICATION OF ROTATIONALLY TRISTABLE COMPLIANT MECHANISMS

Tyler Max Pendleton

Department of Mechanical Engineering

Master of Science

The purpose of this research is to develop the tools necessary to create tristable compliant mechanisms; the work presents the creation of models and concepts for design and a demonstration of the feasibility of the designs through the fabrication of tristable compliant mechanism prototypes on the macro scale. Prior methods to achieve tristable mechanisms rely on detents, friction, or power input; disadvantages to these methods include a high number of parts, the necessity for lubrication, and wear. A compliant tristable mechanism accomplishes tristability through strain energy storage. These mechanisms would be preferable because of increased performance and cost savings due to a reduction in part count and assembly costs. Finite element analysis and the pseudo-rigid-body model are used to design tristable compliant mechanisms. The mechanisms are initially designed by considering symmetrical or nearly symmetrical mechanisms which achieve a stable position if moved in either direction from the initial (fabrication) position, thus resulting in a total of three stable positions. The mechanisms are fabricated and tested in both partially and fully compliant forms, and efforts to miniaturize the mechanism are discussed. The ba-

sic mechanism design is used as a starting point for optimization-based design to achieve tailored stable positions or neutrally stable behavior.

An alternative to fabrication methods commonly used in compliant mechanisms research is introduced. This method integrates torsion springs made of formed wire into compliant mechanisms, allowing the desired force, stiffness, and motion to be achieved from a single piece of formed wire. Two ways of integrating torsion springs are fabricated and modeled, using either helical coil torsion springs or torsion bars. Because the mechanisms are more complex than ordinary springs, simplified models are presented which represent the wireform mechanisms as four-bar mechanisms using the pseudo-rigid-body model. The method is demonstrated through the design of mechanically tristable mechanisms. The validity of the simplified models is discussed by comparison to finite element models and experimental measurements. Finally, fatigue testing and analysis is presented.

Most importantly, this work introduces new tristable mechanism configurations available for use in products: any hinge that would benefit from tristability or the unique motion of the mechanisms could be a candidate. Car hoods, flow regulators, switches, relays, and door hinges are just a few products that may someday incorporate the design of the tristable compliant mechanism.

ACKNOWLEDGMENTS

First of all, I would like to acknowledge the hand of God in this work. I believe that all inspiration and truth comes from Him. I know that without His help, this work would not be possible.

Secondly, I would like to thank my wife for her love and support. She has spent many hours listening and reviewing my writing. She has kept our lives in order. Without her help, this work would have been much more difficult.

I would like to especially thank my graduate advisor, Dr. Brian Jensen for his assistance. I am indebted to him for the countless hours he has assisted me through guidance, support, and literary review. I am grateful for his friendship. Dr. Larry Howell and Dr. Spencer Magleby have also provided helpful advice, literary review, and friendship.

I would like to thank Gary Johns for providing helpful assistance in the finite element modeling of the mechanisms.

I also acknowledge the assistance of Ken Forester, Joseph Jacobsen, and Brian Winder for their help in fabricating many of the mechanisms in this work. Also, special thanks to Kevin Cole for his assistance in experimental design of the force-deflection measurements.

This work was supported by the Nokia Research Center, Dallas, TX.

Table of Contents

List of Tables

List of Figures

Chapter 1

Introduction

1.1 Purpose of This Research

Much study and research has been devoted to bistable compliant mechanisms. There have been many publications on this research, as well as several patents issued. However, little research has been conducted on tristable compliant mechanisms. Prior methods to achieving tristable mechanisms rely on detents, friction, or power input; disadvantages to these methods include a high number of parts, the necessity for lubrication, and wear. The challenge is to make a rotationally tristable compliant mechanism that achieves three stable equilibrium positions without relying on previous methods; this mechanism would be preferable over other types of tristable mechanisms because of increased performance and cost savings due to a reduction in part count and assembly costs.

The purpose of this research is to develop the tools necessary to create tristable compliant mechanisms; the work presents the creation of models and concepts useful for design and a demonstration of the feasibility of the designs through the fabrication of tristable compliant mechanism prototypes on the macro scale. Models which can be used to design tristable compliant mechanisms are developed using finite element analysis and the pseudo-rigid-body model. Although finite element analysis is more accurate than the pseudo-rigid-body model, it is more computationally expensive. The simplified models, based on the pseudo-rigid-body model, are used along with the optimization tools to quickly design mechanisms which have stable positions at specified tailored positions while still meeting specified force and/or stress requirements.

The motivation for this work was a tristable hinge in a hand-held electronic device. Proof-of-concept prototypes were fabricated on a larger scale than of the application. In an effort to miniaturize the mechanisms to the application scale, a new fabrication technique

for compliant mechanisms is developed, a technique which was previously not often used in compliant mechanisms research. This technique employs the bending and of wires into shapes that can be modeled as four-bar rigid-body mechanisms by extending the pseudo-rigid-body model.

The scope of this research was for geometrically symmetric compliant mechanisms modeled as four-bar Grashof mechanisms. However, many of the principles used in the design and modeling of these tristable mechanisms can be applied to other types of mechanisms. The models generated in this work, along with the new fabrication technique for compliant mechanisms research, can be used to synthesize compliant mechanisms for a variety of applications. This chapter defines some of the basic concepts and terms associated with tristable compliant mechanisms.

1.2 Terminology

1.2.1 Mechanisms

A mechanism is a mechanical device used to transfer or transform motion, force, or energy [1, 2]. There are literally thousands, if not millions, of mechanisms that have been designed to perform useful functions. These mechanisms can improve the quality of life for mankind by helping to provide the basic necessities of life as well as entertainment.

Three of the basic needs of humans include food, shelter, and clothing. Thousands of mechanisms have been invented which aid in providing these needs. For example, farm machinery, combined with other advancements, has drastically improved yield efficiency of crops. Thousands of tools and machines which incorporate mechanisms allow the skilled operator to more easily build safe and secure shelters. The first power loom was invented in 1785 by Edmund Cartwright, drastically changing the way clothing was made in the world and allowing the needs of more and more people to be met. Finally, invention of thousands of mechanisms has reduced the amount of time spent in labor and allowed mankind more leisure time, which is also improved by mechanisms. Mechanisms provide entertainment in many ways. For example, roller coasters provide a thrill as they accelerate and jerk the occupant through a designed path. Fishing reels give anglers the ability to catch more and larger fish. Cellular phones, which have mechanisms in the buttons and hinge, pro-

vide a means to communicate virtually anywhere in the world. In short, mechanisms have positively impacted the lives of virtually every human being.

1.2.2 Compliant Mechanisms

Compliant mechanisms differ from rigid-link mechanisms because they perform their function through the deflection of flexible segments rather than through rigid links coupled together through pin joints. Compliant mechanisms are the type of mechanisms most often used in nature. They provide a natural, smooth motion, which is often preferable to rigid, mechanical motion associated with rigid-body mechanisms. For example, bee wings, bird wings, tree branches, leaf stems, fish, and single-celled organisms all take advantage of compliance [3].

There are many advantages of compliant mechanisms, including cost reduction and increased performance. Compliant mechanisms provide cost reduction because multiple parts in a rigid-body mechanism can be replaced with one flexible member; this results in a cost savings in manufacturing and assembly costs. Furthermore, compliant mechanisms can often be fabricated using less expensive manufacturing processes.

Because nature uses compliant mechanisms, it is not surprising that compliant mechanisms, when properly designed, exhibit superior performance to rigid-body mechanisms. The substitution of compliant mechanisms for pin joints can significantly improve the performance of a device because of the reduction or elimination of backlash and friction as well as the need to lubricate the mechanism. This results in a mechanism which is smoother, lighter, more precise, and longer lasting, especially in a harsh environment.

1.2.3 Stability

Multistable mechanisms have two or more stable equilibrium positions, positions which the mechanism will return to if acted upon by only a small force. As the name implies, a bistable mechanism has two stable positions and a tristable mechanism has three stable positions. More formally, the definition of stability can be summarized as follows [4, 5, 6]: a system is in a state of stable equilibrium if small external disturbances cause the system to simply oscillate about the equilibrium state; a system is unstable when a small

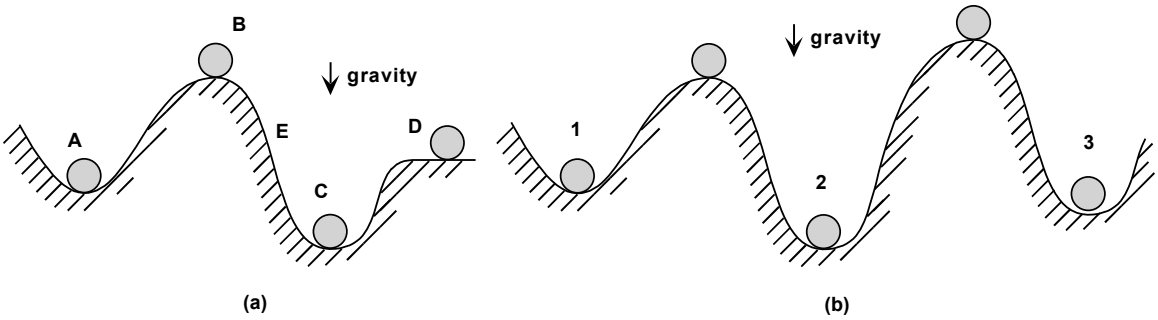

Figure 1.1: Ball on the hill analogy: (a) illustrates the definition of stability. Positions A and C are stable equilibrium positions, B is an unstable position, and D is a neutrally-stable position. (b) Illustrates the potential energy curve of a tristable mechanism.

external disturbance causes the system to diverge from its equilibrium state; and a system is in neutral equilibrium if a small external disturbance causes the system to remain in the disturbed position. This definition is illustrated by the "ball-on-the-hill" analogy (see Figure 1.1) [3]. Ball A is in a state of stable equilibrium; moving the ball from this position and releasing it will result in the ball oscillating about the stable position. Ball B is in a state of unstable equilibrium: moving the ball slightly to the right or left will result in the ball moving to either the stable position of C or A, respectively. Ball D is in a neutrally stable position: any movement of the ball along the plateau will result in the ball staying in the new position. A ball in position E would be in a nonequilibrium state. The ball-on-the-hill analogy can also be used to illustrate another definition of stability: a mechanism has a stable position at a point of local minimum in its potential energy curve. The height of the ball represents the potential energy of the system plotted throughout the range of its motion. The hill represents a local maximum, which is an unstable equilibrium position. A valley represents a local minimum, which, according to the Lagrange-Dirichlet theorem, is a stable equilibrium position [7]. Thus, the potential energy curve can be used as a design tool to predict the stable equilibrium positions of a mechanism. Figure 1.1(b) also shows the ball on the hill analogy for a tristable mechanism.

1.3 Importance of this Research

A wide variety of devices incorporate hinges in their function. Some of these devices make use of a tristable hinge, which traditionally requires a high number of parts and a complex design. The motivation for the research is to design a hinge that is stable in three positions: closed, partially open, and fully open. Potential applications for the tristable mechanism include cell phone hinges, door hinges, car hoods, flow regulators, switches, and relays. Current methods for achieving stability require the use of detents, friction, and/or power input. The use of a rotationally tristable compliant mechanism could drastically reduce the cost of the hinge as a result of a reduction in part count and assembly cost. Furthermore, the performance of the hinge could be improved by a reduction in wear, resulting in prolonged hinge life. The greatest cost savings could be achieved with a fully compliant hinge.

A variety of fabrication techniques have been used in compliant mechanisms research, allowing researchers to fabricate mechanisms both on the macro and micro scale. However, it has been difficult to fabricate small macro-scale compliant mechanisms. Current prototyping methods for compliant mechanisms on the macro-scale largely utilize polypropylene sheets and CNC milling [8]. The methods have proven to be reliable and relatively inexpensive. However, polypropylene has limitations in that it is susceptible to creep; furthermore, the ability to miniaturize mechanisms is limited by the material and fabrication process. By using metals, the issue of creep failure is reduced. Wire forming and metal forming could be employed as new prototyping methods for compliant mechanisms that not only store energy but also constrain motion. The material properties of metals are more reliable, easier to model, and can be improved by heat treatment. Until now, the use of wireforms in compliant mechanisms research has been largely neglected. This work provides researchers of compliant mechanisms with a new fabrication method which, among other advantages, allows the mechanisms to be miniaturized while still maintaining good strength and performance.

1.4 Contributions

Perhaps the most important impact the proposed research will have is the introduction of new tristable mechanism designs available for use in products. It is not difficult to conceive ideas where the tristable mechanism could be incorporated into products; any hinge that would benefit from tristability or the unique motion of the mechanism is a candidate. Car hoods, flow regulators, switches, relays, and door hinges are just a few products that may someday incorporate the design of the tristable compliant mechanism.

The use of the pseudo-rigid-body model, coupled with optimization algorithms, provides designers with a fast, effective tool for synthesizing tristable compliant mechanisms. Using the proper objective function, optimization allows one to design a tristable mechanism with tailored stability locations. A mechanism which exhibits 180 degrees of continuous neutral stability was also designed using these tools.

This work provides the first description of a fabricated tristable compliant mechanism. Previous publication has not described the fabrication of a tristable mechanism. Furthermore, the first fully-compliant and wireform tristable compliant mechanisms are discussed.

A final contribution of this work is new fabrication methods for compliant mechanisms using wire forming and metal forming. These methods may be helpful to others in the field of compliant mechanisms research, allowing new types of compliant mechanisms to be implemented. Until now, CNC milling of polypropylene has been the prototyping method of choice for research. The new fabrication methods reduce the cost of prototypes, increase the ability to miniaturize the mechanism, and facilitate the reduction of thickness and volume.

1.5 Outline of the Thesis

Chapter 2 discusses the foundation that the models presented in this work are based upon: the pseudo-rigid-body model. Chapter 2 also discusses the previous work done in the field of multistable compliant mechanisms, including bistable and tristable compliant mechanisms. Chapter 3 gives a brief review of multistable mechanisms and discusses the design and fabrication of a tristable mechanism using polypropylene. Fully-compliant and

partially compliant versions are discussed. Optimization techniques are also discussed, allowing one to design tristable mechanisms with a wide variety of effects, including specified equilibrium positions and for neutral stability. Chapter 4 discusses the design and fabrication of two different tristable compliant mechanisms which are made of bent wire. Discussion of the performance of the mechanisms as well as a fatigue analysis of the second mechanism is presented. Finally, Chapter 5 summarizes the work as well as provides recommendations for future work in this area of research.

Chapter 2

Background

Compliant tristable mechanisms research is built on the foundation that others have built; without their contributions, this work would not be possible. This chapter discusses key contributions of others which have led to the research of tristable compliant mechanisms. The chapter contains a description of those aspects of the pseudo-rigid-body model which were helpful in this work and a discussion of multistable mechanisms, with particular emphasis on bistable mechanisms.

2.1 Prior to the Pseudo-Rigid-Body Model

Because compliant mechanisms rely on the deflection of members, it is important for a designer of compliant mechanisms to have an accurate understanding of beam deflection behavior. A considerable amount of research has been contributed since Euler described beam deflections mathematically with the well-known Bernoulli-Euler beam equation in 1744 [9]. The location of the end of a cantilever beam loaded with a vertical force at the free end was derived from the Bernoulli-Euler beam equation, with the assumption that the deflection was small and linear. The equation found in most textbooks for vertical beam end deflection is described as

$$y = \frac{Fl^3}{3EI} \tag{2.1}$$

where F is the applied force at the free end, E is the modulus of elasticity of the material, I is the moment of inertia, and l is the length of the beam. Consider the cantilever beam shown in Figure 2.1. Under large, nonlinear deflections, the beam curves such that the location of the end of the beam moves both vertically and horizontally. This makes Equation 2.1 useless to designers of compliant mechanisms because it gives inaccurate in-

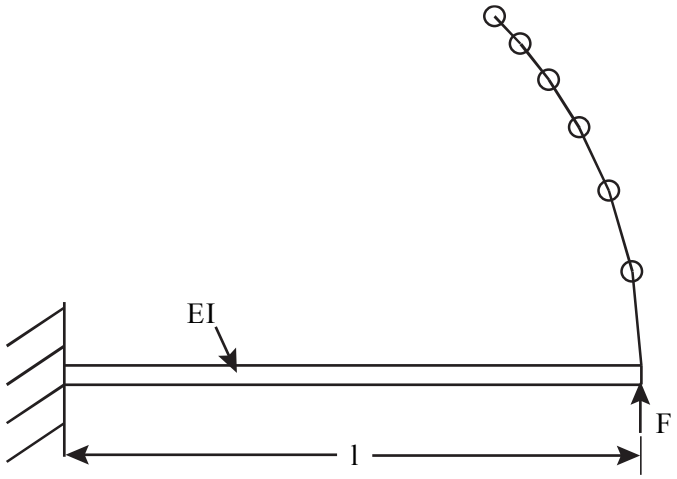

Figure 2.1: The deflection of the end of a flexible cantilever beam with vertical force loading.

formation about the vertical position and no information about the horizontal position of the end of the beam as it is deflected.

In 1945 the Bernoulli-Euler equation was solved using elliptic integrals, allowing for accurate prediction of beam behavior, even for large deflections [10]. However, the solution of these equations is difficult and often computationally expensive. Finite element modeling is also an accurate solution to large beam behavior, but it is too computationally expensive for preliminary design work.

2.2 The Pseudo-Rigid-Body Model

In 1994 Howell and Midha [11] introduced the first pseudo-rigid-body model, which greatly simplified the analysis of large deflections in beams. Since that time, the pseudo-rigid-body model has been developed for many different beam configurations and loading conditions. A comprehensive description of the pseudo-rigid-body model for a variety of different beam configurations and boundary conditions is found in [3]. Fixed-pinned boundary conditions are the only conditions considered in this work; thus, that is the only pseudo-rigid-body model that will be discussed here.

Figure 2.1 shows the beam end deflection path as calculated using elliptic integral solutions. Because the path is nearly circular, the beam can be modeled as a rigid beam

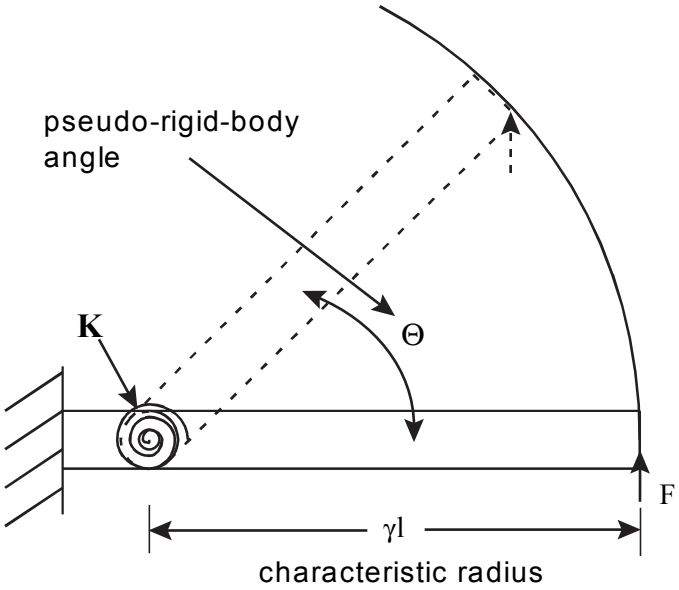

Figure 2.2: The pseudo-rigid-body model of a cantilever beam with a force at the free end.

connected to a pin joint at the center of the deflection path, as shown in Figure 2.2. The radius of the circle, called the characteristic radius, is of length γl, where l is the length of the beam and γ is the characteristic radius factor. For a vertical load, γ was calculated to be 0.8517; this value kept the error to only 0.5% at a beam-end angular deflection of 77 degrees. Exact values are provided by Howell for various directions of beam-end loading, but an average characteristic radius factor $\gamma_{ave} = 0.85$ may be used for any direction with fairly good accuracy; for a fixed-pinned condition, where the force direction is not always known, this greatly simplifies the calculations, though some accuracy is sacrificed.

The stiffness of the beam can be modeled by placing a torsional spring at the pin joint. The stiffness of the beam is

$$K = \gamma K_\theta \frac{EI}{l} \tag{2.2}$$

where K_θ is a scalar dependent upon load direction. An average value of 2.65 for K_θ usually gives good results.

2.3 Grashof's Criterion

The mechanism in Figure 2.3 is a four-link mechanism with link lengths labeled according to length. A four-link mechanism can be categorized according to Grashof's

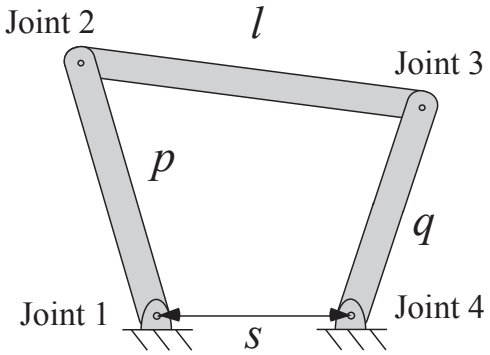

Figure 2.3: A four-link mechanism with links s, l, p, and q, the shortest, longest, and intermediate lengths, respectively.

Criterion [12, 13, 14] by the inequality

$$s + l \leq p + q \tag{2.3}$$

where s is the shortest link, l is the longest link, and p and q are the two intermediate-length links. If the inequality is true, then the mechanism is considered a Grashof mechanism, where full rotation of the links is possible. If the inequality is false, then the mechanism is considered a non-Grashof mechanism and continuous rotation is not possible. The scope of this thesis limits discussion to four-bar Grashof mechanisms which are geometrically symmetric (or nearly geometrically symmetric).

2.4 Factors Governing Bistable Behavior in Compliant Mechanisms

Bistable mechanical devices have recently seen considerable interest. These mechanisms have the advantages that they can maintain two stable states without power input and with high repeatability [15]. Bistable mechanisms have been used in switches, valves, hinges, and many other applications. In addition, there has been a focus on bistable microdevices (see, for example, [16, 17, 18]) for switches, microvalves, and micropositioners. Much of the most recent work has focused on design of bistable devices—in the form of design rules [19, 20] as well as optimization-based approaches [21, 22, 23].

Jensen and Howell [19] propose and prove a theorem which governs the stability of bistable compliant mechanisms modeled as four-bar Grashof mechanisms:

> A compliant mechanism whose pseudo-rigid-body model behaves like a Grashof four-link mechanism with a torsional spring placed at one joint will be bistable if and only if the torsional spring is located opposite the shortest link and the spring's undeflected state does not correspond to a mechanism position in which the shortest link and the other link opposite the spring are collinear.

This theorem can be explained using Figure 2.3. Assuming the four-bar mechanism shown is a Grashof mechanism, placing a torsional spring opposite the shortest link–at either Joint 2 or Joint 3–results in a bistable mechanism. Jensen and Howell's work also presents theorems for non-Grashof and change-point mechanisms and proves these theorems. They present several examples of mechanisms designed using these theorems and the pseudo-rigid-body model. Knowing the factors which govern bistability, and their simplicity, gives the designer freedom to concentrate on other design constraints, such as the motion of the mechanism. While the theorem is limited to four-bar mechanisms with only one torsional spring, Jensen and Howell suggest that the principle can be applied to the design of mechanisms with multiple springs. The effect of additional springs could work for or against bistable behavior. However, depending on the link lengths of the four-bar mechanism, the number of springs, spring locations, and spring stiffnesses, it may be difficult to intuitively predict the stability of the mechanism, even with the knowledge that the theorem gives. The method for analyzing such mechanisms is given in Chapter 3.

Previous work has led to a broad understanding of bistable mechanisms, with many excellent examples in the literature. However, few mechanism examples have been presented that exhibit three mechanically stable positions. One group has claimed to have many tristable designs, but details are not given [23]. The few tristable devices that exist have used friction or mechanical stops to achieve tristability, or they have stacked bistable mechanisms in series to achieve four or more stable positions for the entire system [24]. Disadvantages of the former case include increased wear and decreased performance due to friction. In the latter case, the systems are typically large because they consist of multiple

mechanisms attached together. Just as with bistable mechanisms, numerous applications require three stable states, such as relays, closures, valves or hinges. This thesis presents a compliant mechanism design which has three mechanically stable positions gained through storage and release of elastic energy, not through friction or detents. It is believed that this is the first such mechanism described in the literature.

2.5 Summary

The design of compliant mechanisms is greatly simplified by using the pseudo-rigid-body model, which closely approximates the motion and stiffness of beams–even under large deflections. Since the pseudo-rigid-body model has been successfully used to design bistable compliant mechanisms, it will also be used in the research and design of tristable compliant mechanisms.

Chapter 3

Fundamentals of Tristable Compliant Mechanisms

This chapter presents a mechanically tristable mechanism that uses strain energy storage, rather than friction or detents, to achieve three local minima of potential energy. The mechanism is initially designed by considering symmetrical or nearly symmetrical mechanisms which achieve a stable position if moved in either direction from the initial (fabrication) position, thus resulting in a total of three stable positions. The mechanism is fabricated and tested in both partially compliant and fully compliant forms. In addition, the basic mechanism design can be used as a starting point for optimization-based design to achieve tailored stable positions or neutrally stable behavior.

3.1 Tristable Compliant Mechanism Development

Thus far, few if any compliant tristable mechanisms have been discovered. To facilitate design of tristable mechanisms, a principle governing tristability of symmetric mechanisms was developed. If a symmetric mechanism is bistable in one direction and one of the stable positions occurs at the point of symmetry in an undeflected position, then it will also have a stable position in the other direction. The resulting mechanism has a total of three stable positions, provided the forward and reverse stable positions do not coincide. This principle is based on the definition of geometric symmetry; the principle can be applied to any type of mechanism. This work focuses on the design of symmetric four-link Grashof mechanisms. Note that this principle is not commutative. If a mechanism is tristable, it does not mean that it is symmetric. Thus, symmetric tristable mechanisms are only a subset of all tristable designs.

The symmetric tristable principle is illustrated in Figure 3.1. Note that while the potential energy curve for this example is symmetric about the vertical axis, this symmetry

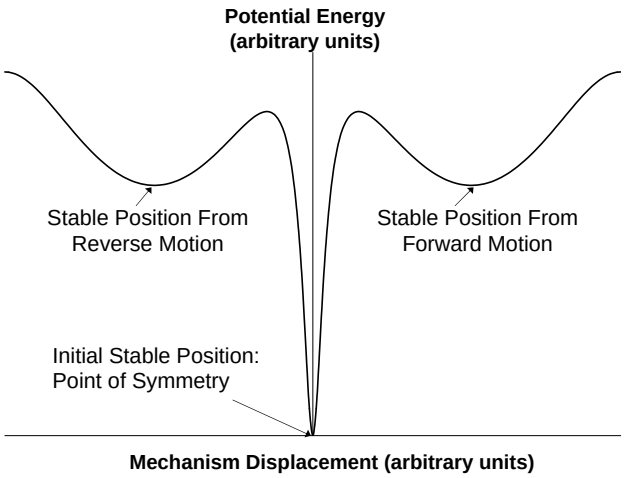

Figure 3.1: Potential energy curve of a symmetric tristable mechanism.

of the potential energy curve is not necessary because the curve may appear differently depending on the generalized coordinate chosen in solving the kinematic equations. Because there is a stable position at the point of geometric symmetry (in the undeflected position) and a stable position along its forward motion, there is a stable position along the reverse motion of the mechanism with equal magnitude of potential energy.

In the past, much of the design and analysis of bistable mechanisms focused on four-bar rigid-link mechanisms with torsional springs at the linkage joints. As was mentioned before, Jensen and Howell proposed four theorems governing bistable behavior of four-bar linkage systems [19]. These theorems are only for four-bar mechanisms with one torsional spring. No rules are proposed for stability of four-bar linkages with two or more torsional springs. Thus, it seems possible that a mechanism with three or more stable positions could be realized with the proper combination of link lengths, undeflected position of the springs, stiffness of the springs, and number of pin joints with torsional springs. The total potential energy curve of a four-bar linkage system with torsional springs at the joints is simply the sum of the individual potential energy curves of each torsional spring joint. This can be described mathematically as

$$V = \frac{1}{2}\sum_{i=1}^{4} k_i \Psi_i^2 \tag{3.1}$$

where V represents the total potential energy of the system (assuming negligible potential energy due to gravity), k_i represents the spring constant of the i^{th} torsional spring joint, and Ψ_i represents the angular displacement from the undeflected position of the i^{th} joint.

In order for a mechanism to be tristable, the summation of the potential energy curves of the individual torsional springs must result in a total potential energy curve with three local minima.

One example of a symmetric four-bar mechanism is a parallel-guiding mechanism. A parallel-guiding mechanism is a symmetric four-bar mechanism which forms a parallelogram, i.e. $r_1 = r_3$ and $r_2 = r_4$. These mechanisms are "change-point" mechanisms because the sum of the length of the shortest and longest links equals the sum of the lengths of the other two links, i.e. $s + l = p + q$. Because past experience has shown that parallel guiding mechanisms can easily be made bistable, it seems a logical starting point for designing a tristable mechanism. Furthermore, shortening link 1 results in a Grashof mechanism ($s + l \leq p + q$), for which the rules governing bistability are well-known.

According to Jensen and Howell, a Grashof mechanism is bistable if and only if a torsional spring is placed at the joint opposite the shortest link [19]. Referring to Figure 3.2, if link 1 is the shortest link, placing a torsional spring at either Joint 2 *or* Joint 3 results in a bistable mechanism. It is possible (but not guaranteed) for a symmetric Grashof mechanism to be tristable by placing torsional springs at Joints 2 *and* 3. The potential energy curves of springs of equal stiffness placed at joints 2 and 3 of a symmetric Grashof mechanism appear in Figure 3.3. The link lengths for this configuration are $r_2 = r_3 = r_4 = 1.1 \times r_1$; spring constants are $k_2 = k_3 = 0.164$ N·m/rad; and links 1 and 3 are horizontal in the undeflected position. Note the two local minima in the energy curve of each spring. The sum of the individual spring energy curves results in a potential energy curve with three local minima. A model which analyzed the kinematics of a four-bar mechanism with torsional springs at the pin joints was used to design the corresponding tristable mechanism. This model also employed the pseudo-rigid body replacement method to design partially and fully compliant versions of the four-bar linkage design. (For details on the pseudo-rigid-body model, see [3].) A second model was developed using finite element analysis to verify the position of the stable positions, the stiffness of the mechanism, and the stress

Table 3.1: Dimensions (in cm) of the original tristable mechanism.

Variable	Description	Units	Value
r_1	Link 1 PRB* Length	cm	12.70
r_2	Link 2 PRB* Length	cm	13.97
r_3	Link 3 PRB* Length	cm	13.97
r_4	Link 4 PRB* Length	cm	13.97
γ	PRB* Parameter	---	0.85
K_Θ	PRB* Parameter	---	2.65
E	Flexural Modulus	GPa	1.379
k_2	Spring Constant, Joint 2	N-m/rad	0.164
k_3	Spring Constant, Joint 3	N-m/rad	0.164

* Abbreviation for Pseudo-Rigid-Body

in the compliant beams. (See Appendix A.1 for details of the batch file used to create the model.) The dimensions of the two mechanisms are included in Table 3.1. (Note: the fully compliant version has the same dimensions as the partially compliant version. The only difference is that the pin joint in the partially compliant version is replaced by a living hinge in the fully compliant version.)

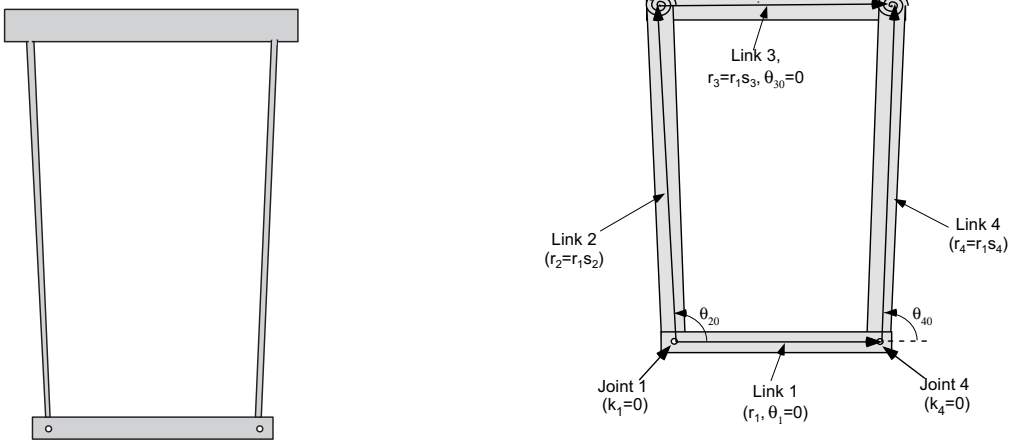

Figure 3.2: Schematic of a pseudo-rigid-body model of a symmetric compliant mechanism.

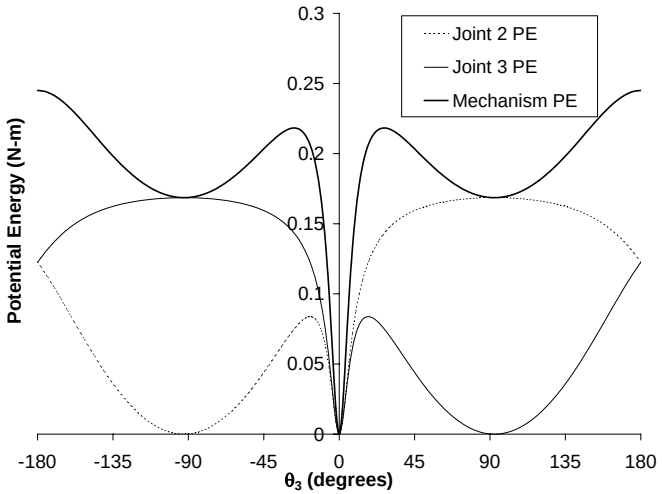

Figure 3.3: Potential energy curves of springs at pin Joints 2 and 3 (link lengths for this configuration are $r_2 = r_3 = r_4 = 1.1r_1$, with angles of 0° for links 1 and 3 when both of the springs are undeflected.)

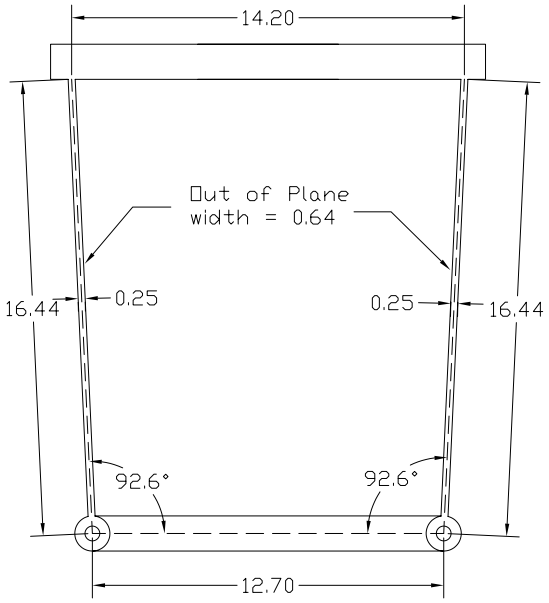

Figure 3.4: Dimensions (in cm) of the original tristable mechanism.

3.2 Fabrication and Testing

Using the dimensions shown in Figure 3.4, mechanisms were machined out of polypropylene sheets using techniques described in [8]. Pictures of the the finished mechanisms appear in Figure 3.5.

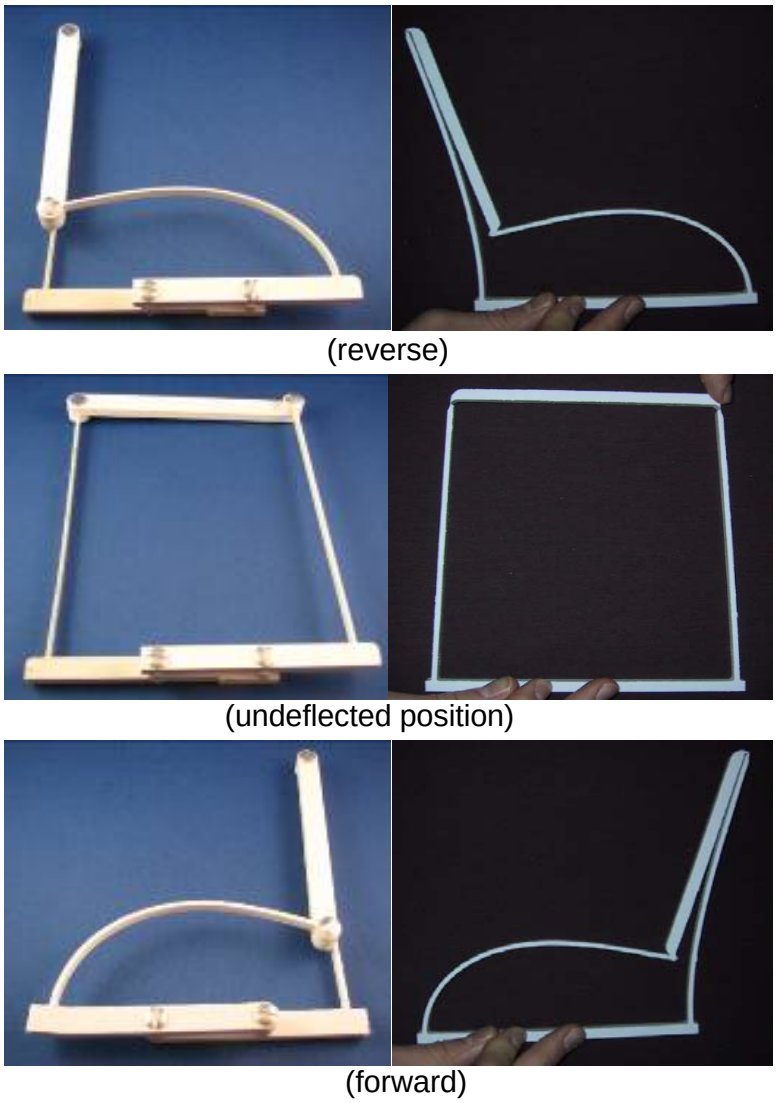

Figure 3.5: Photographs of the partially compliant (left) and fully compliant (right) tristable mechanisms.

The force-displacement curves of the fabricated mechanisms were measured in order to verify the performance of the pseudo-rigid-body model for use in design. The designed mechanisms were modified to provide a convenient way to measure the force-displacement curve of the mechanism. (See Figure 3.6 for images showing the test setup.) A visual alignment guide in the shape of a "T" with a hole in the center was made perpendicular to link 3 at the midpoint, with the hole a distance of approximately 12.7 cm from the center of link 3. A dowel pin was pressed into the hole and attached to a load cell

with a string. The mechanism was then repeatedly photographed while slowly displacing it 180°, taking care to keep the string and load cell parallel to link 3, using the "T" as a visual reference. Also, a second string, approximately 61 cm in length, was attached to lift the mechanism, thus minimizing any friction in the system. The angle of link 3 with respect to link 1 was measured through analysis of the photographs using computer graphics software; the angle and force were measured simultaneously because the digital force readout appeared in the photographs. A plot showing the predicted force-displacement curve from the pseudo-rigid-body model, as well as the measured values, appears in Figure 3.7.

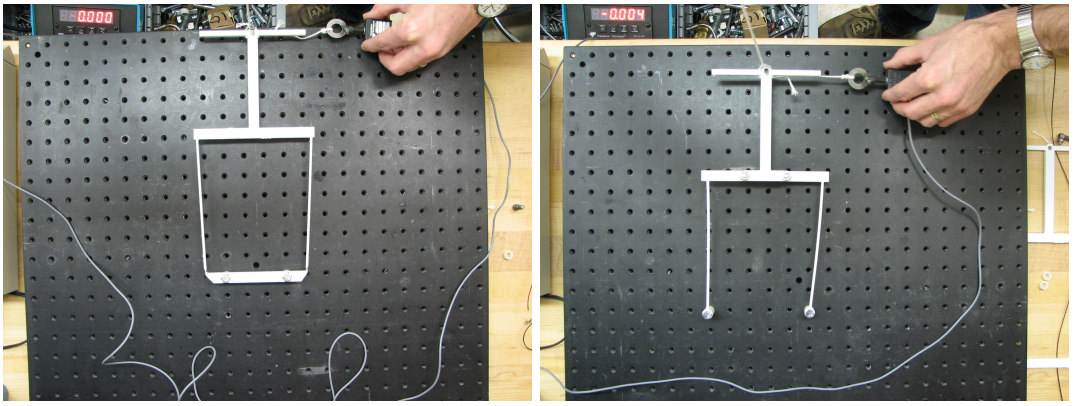

(Fully Compliant) (Partially Compliant)

Figure 3.6: Measuring the force-displacement curve of the partially and fully compliant tristable mechanisms.

The pseudo-rigid-body model greatly facilitated the design of the tristable mechanism; the model simplified the analysis of a complex mechanism, predicting the location of the stable positions and, most importantly, the tristable behavior of the mechanism.

As can be seen in Figure 3.7, there was a difference between the measured values and the values predicted by the models. The largest source of error was associated with the pseudo-rigid-body model. This can be seen in the figures comparing the finite element analysis model predictions and the pseudo-rigid-body model predictions. The discrepancy can be explained by at least two reasons. First, the pseudo-rigid-body parameters were assumed to be constant in order to substantially reduce the computation time; the more accurate method would require updating the changing values of the pseudo-rigid-body pa-

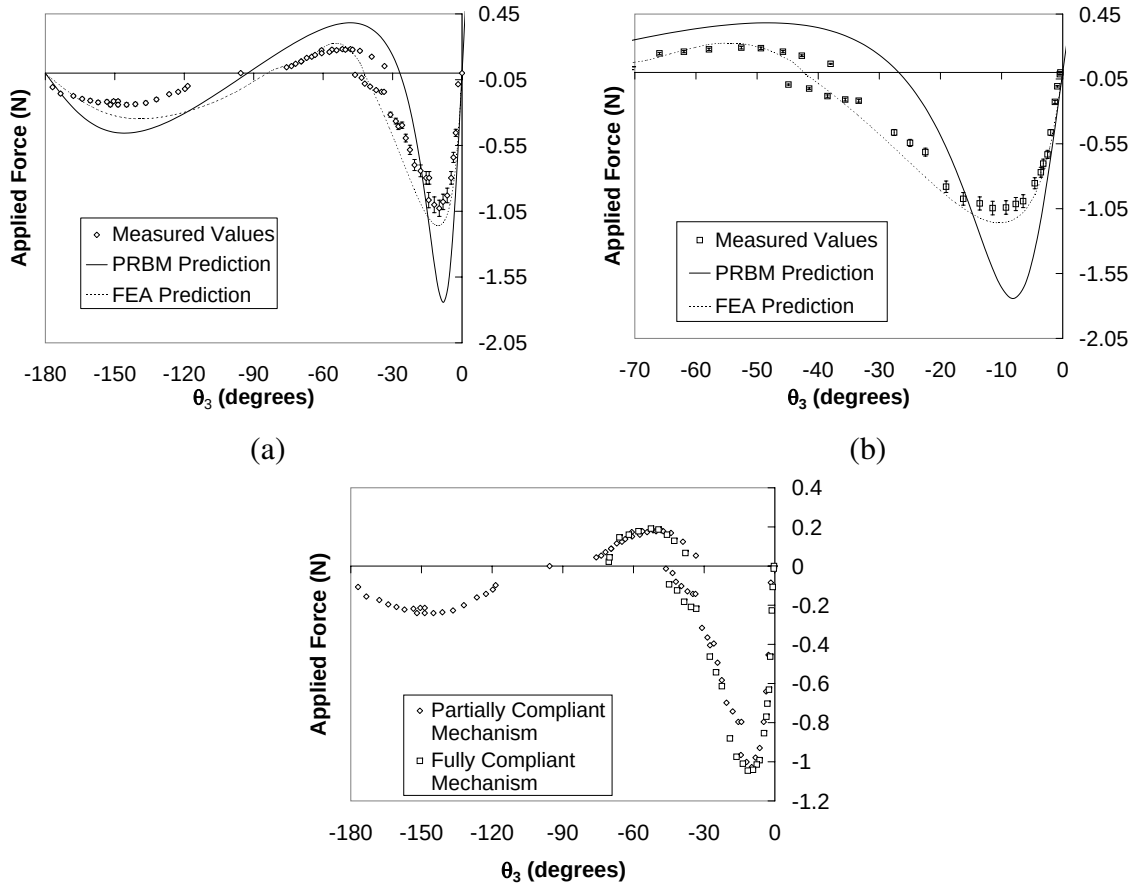

Figure 3.7: A comparison of force-deflection curves, including measured values and values predicted by the pseudo-rigid-body model (PRBM) and the finite element analysis (FEA) model, indicates the usefulness of the models in designing tristable mechanisms. Figures shown are for partially compliant (a), fully compliant (b), and both partially and fully compliant (c) tristable mechanisms.

rameters at every increment of motion. Second, even if the parameters were calculated more accurately, there still would be some error associated with the pseudo-rigid-body model, particularly with high angles of deflection.

The second source of error was associated with the experimental setup. Assumptions made in the model required the applied force to be parallel to link 3, but the load cell and string were not always perfectly parallel to link 3. Maximum error due to this inaccuracy was 5.1 percent. Our models and measurements assume no friction, but it is difficult to completely remove it from the experimental setup. Friction caused some hysteresis in the

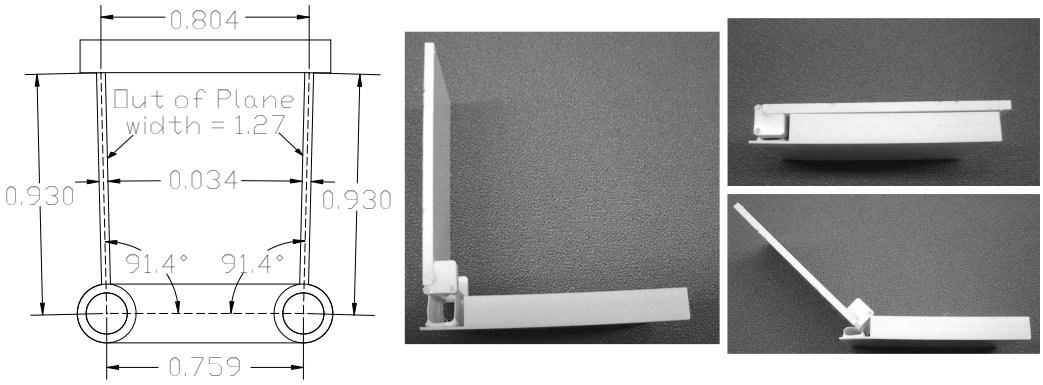

Figure 3.8: Dimensions (in cm) of the smallest tristable mechanism fabricated by milling polypropylene and photographs of the mechanism in a prototype hinge.

measurement; however, the amount of friction in the pin joint seems to be minimal because there is little difference in the measurements of the partially compliant mechanism and the fully compliant mechanism. The long string used to reduce friction may have affected the load cell force measurement if it was not held perfectly normal to the plane of mechanism motion. Finally, while the models assumed no dynamic motion, some dynamic forces may have contributed to error in the measurement.

In conclusion, although there is discrepancy between the measured and predicted values, the trend of the pseudo-rigid-body model is correct. The predicted location of stable positions was accurate to within 4°, and, most importantly, the models performed their purpose of predicting the tristable behavior of the mechanism.

3.3 Miniaturization

Because of the intended application for the tristable mechanism–a hand-held electronic device hinge–efforts were made to miniaturize the mechanism. The smallest mechanism that was successfully fabricated using the same techniques as mentioned before (milling polypropylene sheets) has dimensions listed in Figure 3.8.

This mechanism was successfully implemented in a prototype hinge, as seen in Figure 3.8. However, the mechanism has two inherent problems: first, creep and stress relaxation occurs because the mechanism is in a high-stress state when the hinge is fully-open and fully-closed. Hence, over time the performance of the hinge deteriorates. Second, the

size of the mechanism reached the current lower size limit of the prototyping capabilities of machining polypropylene. Further miniaturization efforts may require different fabrication processes and/or materials.

3.4 Optimization

The pseudo-rigid-body model was used to design a mechanism that was tristable. Because the model predicted the force-deflection curve of the tristable mechanism, the same model might be used to design other mechanisms. Some of these mechanisms include mechanisms with stable positions other than that of the original mechanism and mechanisms with large regions of neutral stability. The design of these mechanisms is straightforward by using commercially available optimization tools, by selecting the proper objective function and constraints, and by using the original configuration as a starting point. For this work, the optimization tools available in Microsoft EXCEL were used.

The model can be used to design tristable mechanisms with a variety of different stable positions, although it may not be possible to create the stable positions in all locations. Figure 3.9 shows the potential energy curves of two tristable compliant mechanisms that were designed to have stable positions in specific locations. The mechanism in Figure 3.9(a) was designed with stable positions at θ_3 =-120, 0, and 120°; Figure 3.9(b) has stable positions at θ_3 =-110, 0, and 98°. The objective function that was used in the optimizations was a minimization of the squares of the derivative of the potential energy curve evaluated at the desired stable positions. In addition, the objective function included a penalty function for having a stable position other than the desired position and a penalty function that the depths of the troughs in the energy curve were at least a certain value. This was done as a means to improve the performance of the mechanism by effectually making it more difficult to change from one stable position to the next, making the stable positions "more stable." Several parameters were used as design variables, including s_2, s_3, and s_4, the scaled pseudo-rigid-body lengths of links 2, 3, and 4, respectively; and t_2 and t_4, the thicknesses of compliant segments represented by links 2 and 4, respectively. The only constraint was that the mechanism be Grashof ($s+l \leq p+q$). Figure 3.9 shows the dimensions of the resulting mechanisms.

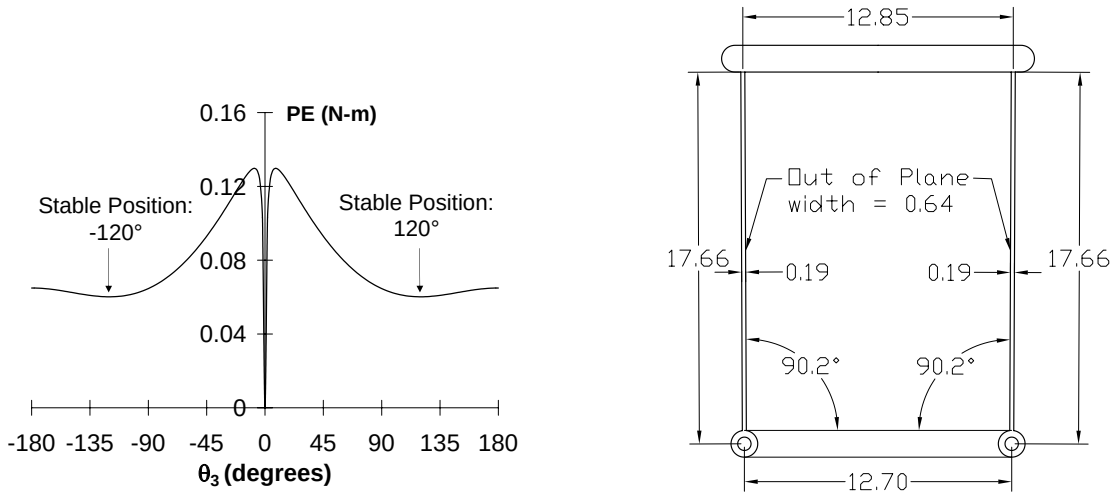

(a)

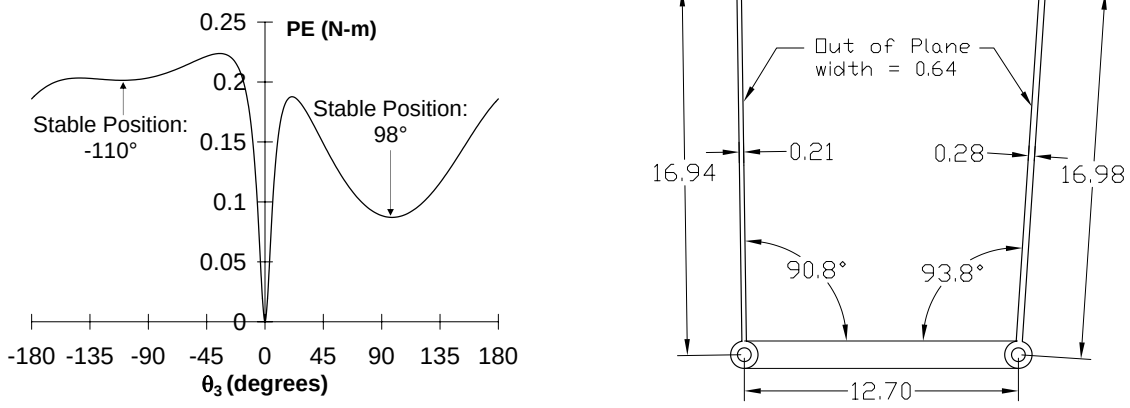

(b)

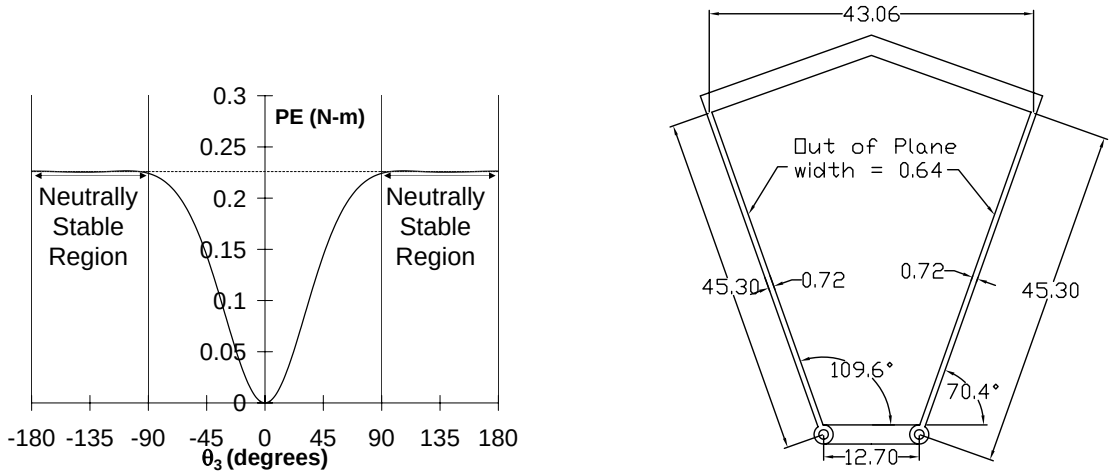

(c)

Figure 3.9: Potential energy curves of compliant tristable mechanisms and their respective dimensions (in cm) with stable positions at (a) θ_3 = -120, 0, and 120°; (b) θ_3 = -110, 0, and 98°; and (c) 180° of neutral stability.

Table 3.2: Dimensions (in cm) of three compliant mechanisms, (a) stable positions at θ_3=-120, 0, and 120°; (b) stable positions at θ_3=-110, 0, and 90°; and (c) 180° of neutral stability.

		Mechanism		
Variable	Units	a	b	c
r_1	cm	12.70	12.70	12.70
r_2	cm	14.40	15.01	37.04
r_3	cm	13.86	12.83	36.91
r_4	cm	14.43	15.01	37.04
k_2	N-m/rad	0.085	0.063	1.409
k_3	N-m/rad	0.211	0.063	1.409

Figure 3.9(c) is the predicted potential energy curve of a mechanism that was designed to have one hundred eighty degrees of continuous neutral stability. The objective function that was used in the optimization was a minimization of the standard deviation of the potential energy curve of the mechanism at discrete points every two degrees in the region $\{-180 \leq \theta_3 \leq -90\}$. Because the mechanism was assumed to be Grashof and symmetric, the inclusion of the region from $\{90 \leq \theta_3 \leq 180\}$ in the objective function was not necessary. The constraints chosen were of symmetry ($r_2 = r_4$ and $t_2 = t_4$), and that the mechanism be Grashof ($s + l \leq p + q$). These constraints reduced the number of design variables to only two, which facilitated finding an optimum. The design variables were s_2 and s_3, which when multiplied by the length of r_1 resulted in the pseudo-rigid-body lengths r_2 and r_3 of the four-bar mechanism. The values of s_2 and s_3 were allowed to vary between 1.1 and 5. The spring constants were held constant during the optimization. Once the optimally-shaped potential energy curve was obtained, it was then easily scaled by changing the values of the thickness and out-of-plane width of the compliant members represented by links 2 and 4; the values were chosen such that the maximum bending stress of the mechanism did not exceed the yield stress of the material. Figure 3.9 shows the dimensions of the resulting mechanism.

3.5 Conclusion

This work represents the design and fabrication of the first tristable compliant mechanism which gains stability through strain energy stored in the members of the mechanism. The measured values of the force-displacement curve of the mechanism closely follow the model that was used to design the mechanism. The trends of the force-displacement curve as well as the location of the stable positions are accurate, allowing use of the model in optimization-based design to achieve a wide variety of effects.

The tristable mechanism has a pseudo-rigid-body model that is a Grashof mechanism with torsional spring joints at two pin joints only. Future research will focus on the factors governing tristability. There may be many other configurations, such as non-Grashof or change point mechanisms, which produce tristable mechanisms. Thus, more research should be conducted exploring how link lengths, undeflected position of the springs, stiffness of the springs, and number of pin joints with torsional springs affect tristability. More concrete theorems governing tristability could give a designer much more understanding and design freedom.

Chapter 4

Wireform Compliant Mechanisms

This chapter presents an approach for integrating torsion springs made of formed wire into compliant mechanisms. In this way the desired force, stiffness, and motion can be achieved from a single piece of formed wire. It also allows an alternative fabrication method for making compliant mechanisms. Two ways of integrating torsion springs are fabricated and modeled: helical coil torsion springs and torsion bars. Because the mechanisms are more complex than ordinary springs, simplified models, which aid in design, are presented which represent the wireform mechanisms as mechanisms using the pseudo-rigid-body model. The method is demonstrated through the design of a mechanically tristable mechanism. The validity of the simplified models is discussed by comparison to finite element models and, in the case of the torsion bar mechanism, to experimental measurements. A fatigue analysis of the torsion bar mechanism is presented and discussed.

4.1 Introduction

For many reasons, compliant mechanisms are often manufactured using polymers [8]. Advantages of polymers include low process and material costs, resistance to corrosion, self-lubrication, and a relatively high strength-to-stiffness ratio. However, metal is preferable when it is important to eliminate creep and stress relaxation as well as in high-temperature applications. Furthermore, the material properties of metals are more reliable, better-understood and more easily modeled. Finally, it is often easier to reliably fabricate small mechanisms with metals. Herring et al. gives a thorough discussion on manufacturing processes for metal compliant mechanisms [25]. Metal compliant mechanisms have been fabricated using bending of sheets [26, 27], laser cutting [28], stamping [29, 30],

wire EDM [31, 32, 33], and machining [30]. This paper extends available manufacturing techniques by demonstrating compliant mechanisms formed from wire.

4.2 Model of Wireform Mechanism With Coiled Torsional Springs

Compliant mechanisms are often modeled using the pseudo-rigid-body model, which represents deformable segments as rigid links joined by pin joints. (For details on the pseudo-rigid-body model, see [3].) The pseudo-rigid-body model can be used to design a compliant mechanism by using rigid-body mechanism theory. The resulting pseudo-rigid-body design is then translated into the corresponding compliant mechanism. It is not unusual for one pseudo-rigid-body model to correspond to several compliant mechanisms with that behavior. Here an additional class of compliant mechanisms is proposed for translation from the pseudo-rigid-body model to compliant mechanisms. It is proposed to design a one-piece wireform mechanism in which the wire is coiled several times at the points where the pseudo-rigid-link mechanism has torsional springs at pin joints. The pseudo-rigid-body model uses the length, moment of inertia, and material properties of the compliant beam to calculate the torsional stiffness of the spring that represents the bending stiffness of the beam. Using equations for torsional coil springs, a stiffness model was developed which used the number of coils, diameter of coils, as well as the moment of inertia and material properties of the wire.

The spring constant of each of the spring joints was calculated from the equation for the spring constant of a helical coil torsion spring, given by Shigley et al. [34] as

$$k' = \frac{d^4 E}{10.8 D N_a} \tag{4.1}$$

where k' represents the spring constant per coil, d represents the diameter of the wire, E represents the Young's modulus of the material, D represents the mean coil diameter, and N_a represents the number of active coils,

$$N_a = N_b + \frac{L_1 + L_2}{3\pi D} \tag{4.2}$$

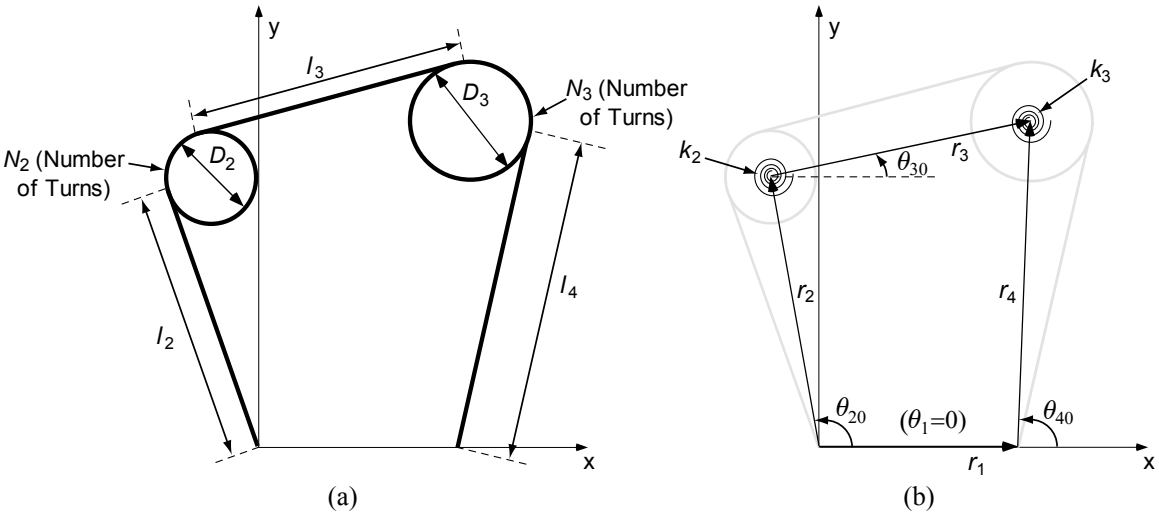

Figure 4.1: Schematic (a) of the wireform tristable mechanism and (b) its model.

where N_b is the number of body turns and L_1 and L_2 are the tangential leg lengths of the spring.

The spring constant per radian is calculated by dividing by 2π radians and substituting Equation (4.2) into Equation (4.1), resulting in

$$k = \frac{d^4 E}{67.8D(N_b + \frac{L_1+L_2}{3\pi D})} \tag{4.3}$$

Figure 4.1 shows the geometry of a mechanism modeled as a four-link mechanism with torsional springs at two adjacent pin joints. The geometry of the mechanism is substituted into Equation (4.3), resulting in spring constants for Joints 2 and 3

$$k_2 = \frac{d^4 E}{67.8D_2(N_2 + \frac{l_2+\frac{l_3}{2}}{3\pi D})} \tag{4.4}$$

$$k_3 = \frac{d^4 E}{67.8D_3(N_3 + \frac{l_4+\frac{l_3}{2}}{3\pi D})} \tag{4.5}$$

where N_2 and N_3 represent the number of active coils in Joints 2 and 3, respectively; and l_2, $\frac{l_3}{2}$, and l_4 represent the tangential leg lengths.

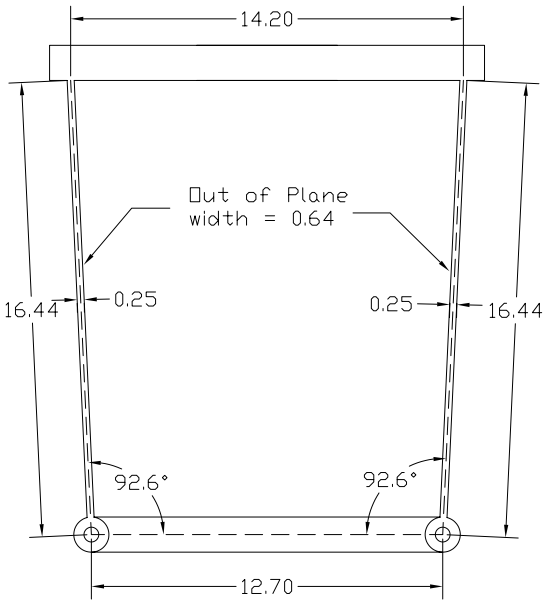

Figure 4.2: Dimensions of the original tristable mechanism, fabricated by milling polypropylene sheets.

A finite element model was also created to predict the stable positions, stiffness, and stress of the mechanism. (For details of the finite element model, see Appendix A.2)

4.3 Fabrication of the Helical Coil Spring Tristable Mechanism

Chapter 3 discussed the design of fully-compliant tristable mechanisms made of polypropylene. These mechanisms, modeled as four-bar mechanisms using the pseudo-rigid-body model, were fabricated on the order of approximately 12.7 cm per link (see Figure 4.2).

Because of a need to fabricate the tristable mechanisms on a scale approximately 50 times smaller than the mechanism in Figure 4.2, efforts were made to substitute wire for polymer materials; this scale was beyond the limits of the customary fabrication technique of milling polypropylene sheets [8]. Two mechanisms were designed using both the pseudo-rigid-body model and finite element analysis. One mechanism (Figure 4.3) was fabricated at approximately five times smaller than the tristable mechanism made of polypropylene; the other mechanism (Figure 4.4) was fabricated at approximately thirty-

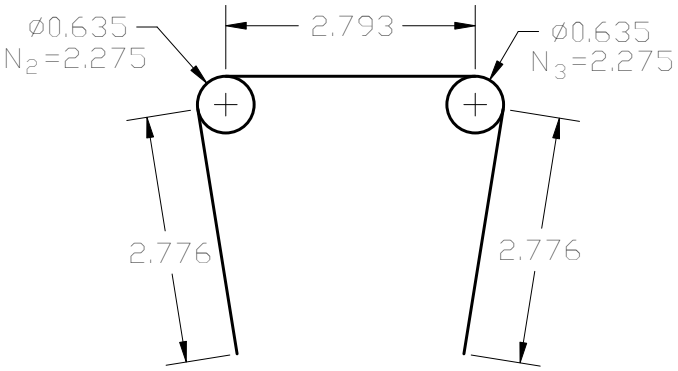

Figure 4.3: Dimensions (in cm) of the large coil mechanism.

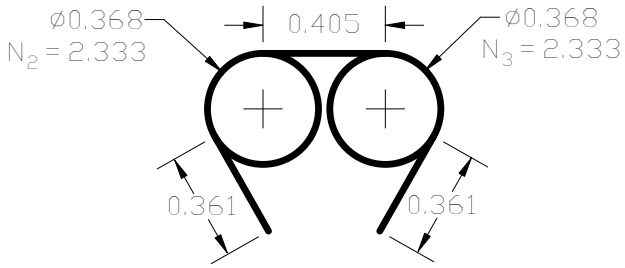

Figure 4.4: Dimensions (in cm) of the small coil mechanism.

five times smaller, showing the importance and practicality of the fabrication technique. Figure 4.5 compares the predicted force-deflection curves of the mechanisms using the simple model and finite element analysis, with the simplified model parameters listed in Table 4.1. Figure 4.6 contains photographs of the fabricated mechanisms in their three stable positions.

Table 4.1: Model parameters of the two fabricated coil mechanisms.

	Small Coil	Large Coil
d (mm)	0.376	0.376
r_1 (cm)	2.540	0.368
r_2 (cm)	2.794	0.405
r_3 (cm)	2.794	0.405
r_4 (cm)	2.794	0.405
k_2 (N-cm/rad)	0.636	0.304
k_3 (N-cm/rad)	0.636	0.304
θ_{20}	92.6°	92.6°
θ_{30}	0.00°	0.00°
θ_{40}	87.4°	87.4°

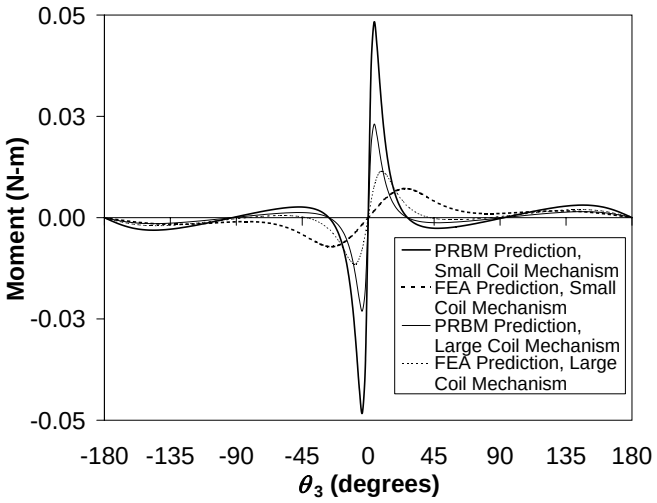

Figure 4.5: Comparison of the predicted moment-deflection curves of the two coil mechanism models, the pseudo rigid body model (PRBM) and the finite element analysis (FEA) model.

As can be seen in Figure 4.5, the force-deflection curves predicted by the pseudo-rigid-body model (PRBM) and the finite element analysis (FEA) model are quite different. The force-deflection curve predicted by the simple model is much steeper, has greater magnitude, and predicts different stable positions than does the prediction by the finite element model. The finite element simulation demonstrated that as the mechanism is rotated, the coils deflect such that they no longer lie on top of each other, becoming stretched out. This phenomenon, which is especially inherent to mechanisms with very thin wires, was not accounted for in the simple model. However, as the wire diameter increases, the error between the simple model and the finite element model decreases, though never close enough for the simple model to accurately predict the force-deflection curve. Another reason for the discrepancy between the models may be attributed to the fact that the coil diameter and leg lengths change with mechanism displacement, a phenomenon that was accounted for by the simple model only in the stiffness; it was assumed that the phenomenon would have negligible effect on the pseudo-rigid-body lengths of the four-bar mechanism in the simple model.

(Reverse)

(Undeflected)

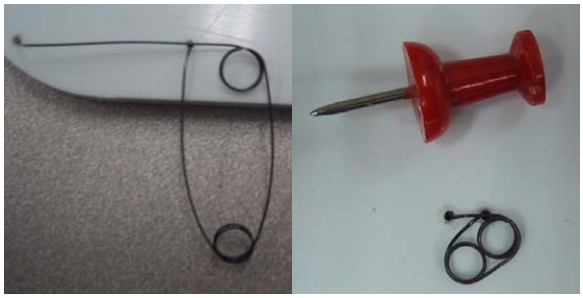

(Forward)

Figure 4.6: Photographs of two different tristable compliant mechanisms with torsional springs.

While the simple model lacks some accuracy in the prediction of the force-deflection curve, it is still valuable as a design aid as it can be used to predict the quantity and locations of stable positions of devices with larger wire diameters.

4.4 Model of Torsion Bar Wireform Mechanism

An alternative type of torsion spring to a helical coil torsion spring is a torsion bar. According to an expert spring manufacturer [35], the torsion bar configuration is easier to manufacture than the coiled configuration. Figure 4.7 shows a mechanism with torsion bars which can be modeled using the same pseudo-rigid-body model as was used before

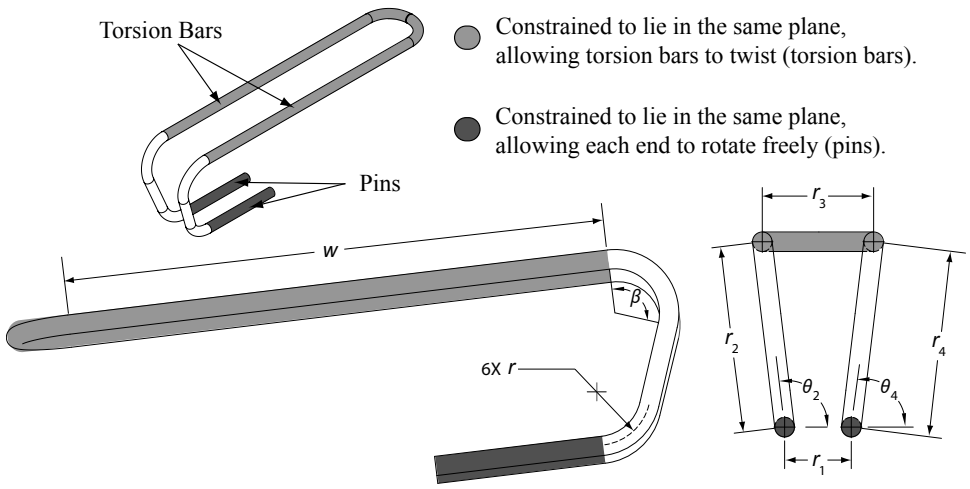

Figure 4.7: Isometric, auxiliary, and front views of the torsion bar mechanism, showing model parameters. (Shading is added for clarity to describe how the mechanism works.)

(see Figure 4.1). A slot milled in the same shape as the mechanism, together with a plate covering (effectively a square hole), constrains the long, straight sections of the mechanism (the torsion bars) and the section joining them; the wire ends are constrained in circular holes. Thus, the mechanism is constrained such that when r_3 is rotated with respect to r_1, the sections marked r_2, r_3 and r_4 are put into bending while the long, straight segments are put into torsion. Referring to Figure 4.1, the stiffnesses of Joints 2 and 3 are related to the stiffnesses of the portions of the mechanism in both bending and torsion, so an equivalent spring stiffness is calculated. The stiffness of the portion in bending is assumed to act in series with and in the same plane as the stiffness in torsion, with the equivalent springs located at Joints 2 and 3. The derivation of the equivalent spring constants follows.

A beam with circular cross-section in pure torsion has a spring constant of [36]

$$k_T = \frac{GI_P}{L} \tag{4.6}$$

where G is the shear modulus of elasticity, I_P is the polar moment of inertia, and L is the length of the beam. The length of the mechanism in torsion is assumed to be equal to the sum of the out-of-plane width of the mechanism and the circumferential length of the mean

bend radii (see Figure 4.7)

$$L_T = w + r(\beta + \frac{\pi}{2}) \tag{4.7}$$

Substituting Equation (4.7) for the length in torsion, $G = \frac{E}{2(1+\nu)}$ for the shear modulus of elasticity, and $I_P = \frac{\pi d^4}{32}$ for the polar moment of inertia of a beam with solid circular cross-section, the stiffness can be expressed as

$$k_T = \frac{E\pi d^4}{64[w + r(\beta + \frac{\pi}{2})](1+\nu)} \tag{4.8}$$

According to the pseudo-rigid-body model [3], the stiffness of a cantilever beam in bending is

$$k = \gamma K_\theta \frac{EI}{L} \tag{4.9}$$

where γ is the characteristic radius factor, K_θ is the nondimensionalized torsional spring constant, E is Young's modulus, I is the moment of inertia of the beam, and L is the beam length. Constant values of $\gamma = 0.85$ and $K_\theta = 2.65$ are assumed in order to simplify the calculations, and substitute $I = \frac{\pi d^4}{64}$ for the moment of inertia, resulting in the spring constant for the portion of the mechanism in bending,

$$k_{bending} = 0.0352 \frac{E\pi d^4}{L} \tag{4.10}$$

Equivalent spring constants, k_2 and k_3, are assumed to act in the same plane at Joints 2 and 3 (see Figure 4.1(b)). They can be calculated by adding the spring constants for the respective portions of the mechanism (k_T and $k_{bending}$) together in series. The length of the mechanism in bending L is assumed to be equal to $r_2 + \frac{r_3}{2}$ and $r_4 + \frac{r_3}{2}$ for k_2 and k_3, respectively.

$$k_2 = k_{eq} = \frac{1}{\frac{1}{k_T} + \frac{1}{k_{beam}}} = \frac{1}{\frac{64(w + r(\beta + \frac{\pi}{2}))(1+\nu)}{E\pi d^4} + \frac{28.41(r_2 + \frac{r_3}{2})}{E\pi d^4}} \tag{4.11}$$

$$k_3 = k_{eq} = \frac{1}{\frac{1}{k_T} + \frac{1}{k_{beam}}} = \frac{1}{\frac{64(w + r(\beta + \frac{\pi}{2}))(1+\nu)}{E\pi d^4} + \frac{28.41(r_4 + \frac{r_3}{2})}{E\pi d^4}} \tag{4.12}$$

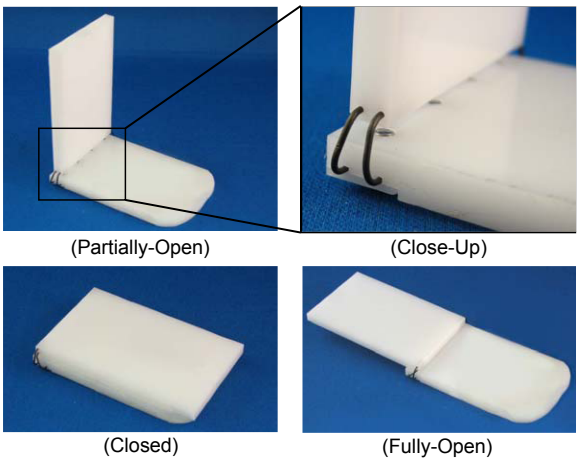

Figure 4.8: Photographs of the torsion bar mechanism prototype hinge.

Finally, these stiffnesses are used along with the equations of a four-bar mechanism with link lengths as shown in Figure 4.7 to predict the motion and stiffness of the torsion-bar mechanism.

A finite element model of the mechanism was also created to predict the position of the stable positions, the stiffness, and the stress in the mechanism. (See Appendix A.3 for details of the batch file used to create the model.) The force-deflection curve predictions for both models are shown in Figure 4.10.

4.5 Fabrication and Testing

Figure 4.8 shows photographs of the torsion bar tristable mechanism in a prototype hinge. This mechanism was fabricated at a scale fifty times smaller than the original mechanism fabricated from polypropylene (see Figure 4.2).

The force deflection curve was measured (see Figure 4.9) to demonstrate the accuracy and usefulness of the models in design. The stable position of the undeflected mechanism was predicted to within two degrees, and the other two stable positions were predicted to within the measurement uncertainty. Figure 4.10 shows the measured and predicted force-deflection curves. As can be seen, the models agree well, especially for predicting the local maxima of the curves. The maximum difference between the two models, divided by the maximum reaction force, is 18.5% while the percent error at the maximum

force is only 0.25%. The magnitude of the predicted maximum force is 41% higher than the measured maximum force. This discrepancy can likely be attributed to the clearance in the slot of the hinge. A more accurate finite element analysis model allowed the mechanism to deflect to the sides of the slot. The results of this model are seen in Figure 4.10. The increased accuracy of the predicted unstable positions and the magnitude of the force curve provides evidence that the discrepancy between the measured values and the models is due to the clearance in the slot. Reducing the clearance or using an overmolding process would stiffen the mechanism such that the models would accurately predict the force-deflection curve.

4.6 Fatigue of Wireform mechanisms

One of the challenges in the field of compliant mechanisms is ensuring adequate fatigue life of the mechanisms. Much more research and testing results are available for metals, especially ferrous metals, than for polymers. Thus, if one treats the mechanisms as springs, one advantage of the wireform mechanisms is there is much more information available to predict the fatigue life. The following is a description of fatigue life of the mechanism incorporating torsion bars.

In order to predict the fatigue life of the mechanism, it is important to know the stresses that the mechanism undergoes. The stress in the torsion bars is predicted using the standard equation for shear stress in a circular cross-section beam in pure torsion,

$$\tau_{max} = \frac{Tr}{J} \tag{4.13}$$

where T is the applied torque, r is the radius of the cross-section of the beam, and J is the polar moment of inertia. Substituting $k_\tau \psi_i$, (where ψ_i represents the angular displacement from the undeflected position of the i^{th} joint) as well as the polar moment of inertia for the circular torsion bar, results in

$$\tau_{max} = \frac{16 k_\tau \psi_i}{\pi d^3} \tag{4.14}$$

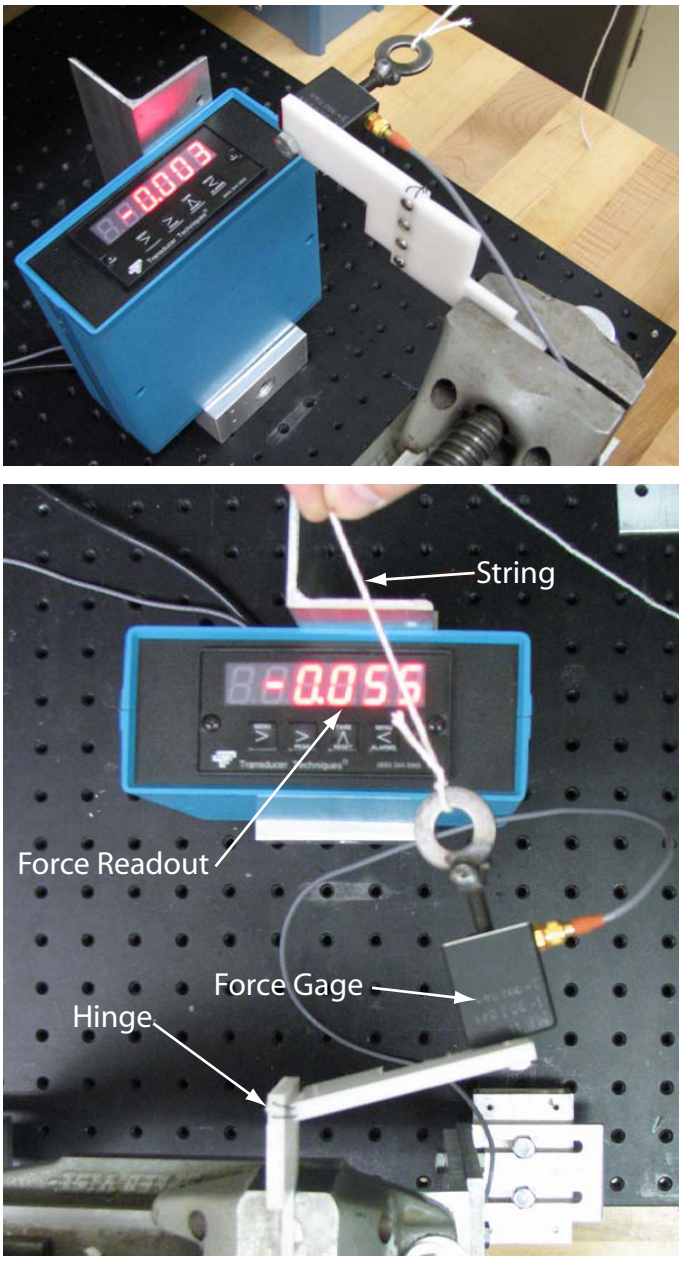

Figure 4.9: Experimental setup for force-deflection measurements of the compliant tristable torsion bar mechanism.

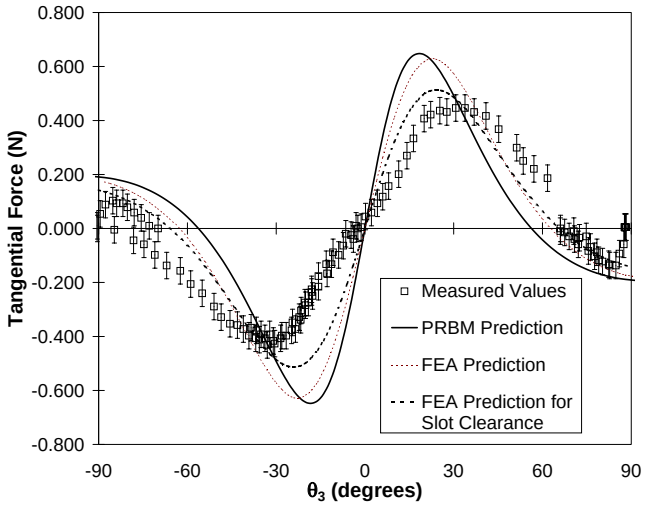

Figure 4.10: Force-deflection curves comparing the measured values to the values predicted by the models.

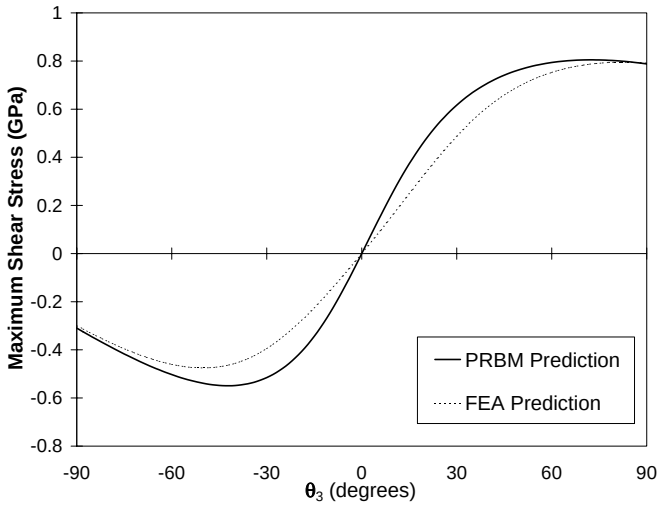

Figure 4.11: Maximum shear stress in the torsion bar section of the mechanism.

Figure 4.11 compares predicted maximum shear stress in the torsion bar section of the mechanism. The simplified model predicts the stress fairly well, especially considering the complex geometry of the mechanism.

The stress in the portion of the mechanism in bending is equal to

$$\sigma_{max} = \frac{Mc}{I} \tag{4.15}$$

where M is the applied moment, c is the distance to the neutral axis, and I is the moment of inertia. Substituting $k_\tau \psi_i$ for M, $\frac{d}{2}$ for c and $\frac{\pi d^4}{64}$ for I,

$$\sigma_{max} = \frac{32 k_\tau \psi_i}{\pi d^3} \tag{4.16}$$

This equation assumes that the portion in bending does not deflect, which is not a valid assumption. An even more accurate prediction for the maximum bending stress subtracts the maximum deflection angle for a cantilever beam with a force at the end from ψ_i

$$\psi_i^* = \psi_i - \frac{FL^2}{2EI} \tag{4.17}$$

From the Free-Body Diagram of the mechanism, it is known that $FL = k_{eq} \psi_i$. Substituting for this and I,

$$\psi_i^* = \psi_i - \frac{32(k_{eq} \psi_i)(r_2 + \frac{r_3}{2})}{E \pi d^4} \tag{4.18}$$

Finally, the substitution ψ_i^* into Equation 4.16 is made. The predicted maximum bending stress for the simplified model as well as the finite element model are shown in Figure 4.12. Again, the simplified model is fairly accurate in predicting the stress as the mechanism is rotated. Discrepancy can be explained, at least in part, by the assumption that the reaction force at the pin joint acts tangential to the section in bending; axial loading is neglected.

Extensive finite element analysis indicated that the maximum Von Mises stress (Figure 4.13) occurred in the bend, where the bending stress and the shear stress due to torsion combine. A fatigue analysis of the mechanism was made for failure in the three cases described above: failure in torsion in the torsion bar, failure in bending in sections r_2 and r_4, and failure in the bend due to combined bending and torsion. Because this mechanism is essentially a spring, the procedure for fatigue failure of springs described by Shigley et al. was used [34]. Table 4.2 lists the model prediction for fatigue failure in each section of the mechanism, as well as the results of actual fatigue testing. The predicted number of hinge cycles to failure using the Modified Goodman equation was 1519, and the predicted location of failure was at the beginning of the bend, on the end closest to the section in bending. The torsion bar mechanism was fatigue tested twice in a machine and once by hand. Actual

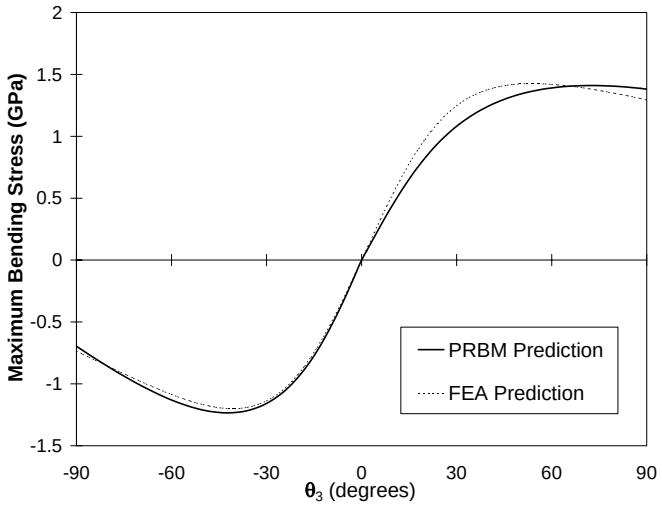

Figure 4.12: Maximum bending stress in the torsion bar section of the mechanism.

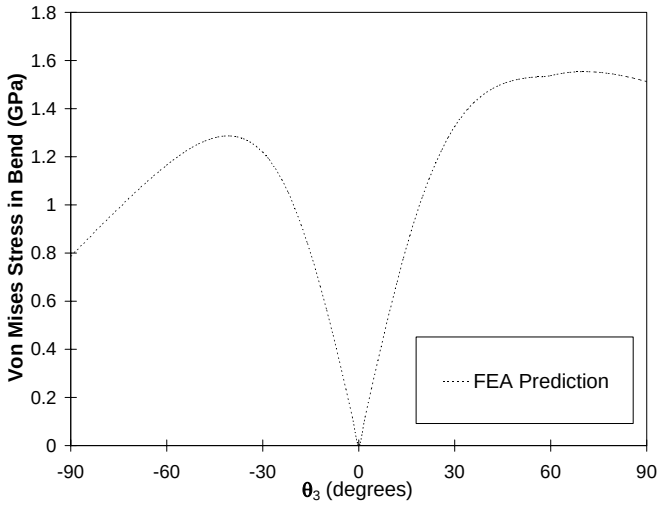

Figure 4.13: Von Mises stress in the bend between the sections in bending and torsion of the mechanism.

test results, for the three fatigue failures, gave an average of 1491 and a standard deviation of 790 hinge cycles. The failure location for each test was at the point of highest stress as predicted in the finite element analysis. Testing validated the fatigue model because the model predicted the location of failure and the number of cycles to failure very closely.

Table 4.2: Fatigue predictions for three critical locations of the mechanism as well as actual test results.

Model Prediction		Testing	
Location	Cycles to Failure	Test	Cycles to Failure
Torsion Bar	3,808	1-Machine	1,027
Leg	2,698	2-Machine	1,042
Bend	1,519	3-Hand	2,404

4.7 Conclusion

This work demonstrates an alternative to fabrication methods commonly used in compliant mechanisms research, allowing compliant mechanisms to be fabricated on a scale that previously has been difficult to achieve. Simple and useful models have been developed to aid others wishing to use these methods to create reliable, small-scale compliant mechanisms. A mechanism was successfully created which allowed for the fabrication of a prototype hinge. Other areas of applicability for compliant mechanisms on this scale (which may or may not require multistability) should be explored, including valves, switches, and hinges.

Chapter 5

Conclusions and Recommendations

5.1 Conclusions

This work represents the design and fabrication of the first tristable compliant mechanism which gains stability through strain energy stored in the members of the mechanism. Models were developed to predict the behavior of the devices and were essential in the design of the tristable mechanisms. The models accurately predict the tristable nature of the mechanisms and the location of the stable positions, allowing one to use the models to design tristable compliant mechanisms and in optimization-based design to achieve a wide variety of effects.

This work also demonstrates an alternative to fabrication methods commonly used in compliant mechanisms research, allowing compliant mechanisms to be fabricated on a scale that previously has been difficult to achieve. Simple and useful models have been developed to aid others wishing to use these methods to create reliable, small-scale compliant mechanisms. A mechanism was successfully created which allowed for the fabrication of a prototype tristable hinge. A history of the development of the prototype is given through photographs in Appendix B.

5.2 Recommendations

5.2.1 Further Design Work

Because the tristable torsion bar mechanism had relatively low fatigue life, it is recommended that further design work be done to improve the reliability and strength of the tristable hinge. A redesign of the tristable torsion bar mechanism to reduce the stress in the

mechanism would include thickening the wire diameter and lengthening the torsion bars; this would strengthen the mechanism while maintaining the stiffness of the mechanism.

Appendix B shows a tristable compliant mechanism which was fabricated from sheet metal. Further development of this concept may result in a tristable hinge which has superior performance to any of the designs presented in this work.

5.2.2 Tristability Theory

The tristable mechanism described in this thesis has a pseudo-rigid-body model that is a symmetric or nearly-symmetric Grashof mechanism with torsional spring joints at two pin joints. Future research should focus on the factors governing tristability. There may be many other configurations, such as non-Grashof or change point mechanisms, which produce tristable mechanisms. Thus, more research should be conducted exploring how link lengths, undeflected position of the springs, stiffness of the springs, and number of pin joints with torsional springs affect tristability. Furthermore, compliant mechanisms modeled as non-four-bar mechanisms should be analyzed for the possibility of more tristable designs. More concrete theorems governing tristability for a variety of mechanisms could give a designer much more understanding and freedom in the design of tristable compliant mechanisms.

5.2.3 Further Product Application

Other areas of applicability for tristable compliant mechanisms should be pursued. Designers may apply the tools described in this work to design compliant tristable mechanisms to replace traditional-type mechanisms and, as mentioned before, improve performance and decrease cost. Furthermore, the wireform technique of fabricating compliant mechanisms should be considered when designing mechanisms on the small macro-scale (which may or may not require multistability); examples may include valves, switches, and hinges.

Appendix A

Ansys Batch Files

This appendix contains the batch files used in the design and analysis of three types of tristable mechanisms: the cantilever beam, coil, and torsion bar. The code presented is for the Ansys finite element software.

A.1 Tristable Mechanism Fabricated From Polypropylene

```
!================================================================
=============== ! ! polypropylene_tristable.txt !    ANSYS
Batch File !    Created by Tyler Pendleton,  24 June 2005 !
!================================================================
=============== ! FINISH /CLEAR /TITLE,  Stresses in beam of
tristable mechanism /PREP7 !
!================================================================
=============== ! !                    INPUT PARAMETERS !
!================================================================
===============
!--------------------------------Geometry-------------------------
---------------
!Variable Description Units
!---------------------------
r1=0.145 !length of link 1  inches
s2=1.8 !link 2 mutiplier ------
s3=1.67 !link 3 multiplier ------
s4=1.8 !link 4 multiplier ------
w=1.5 !out-of-plane width,each link inches
t2=.003 !thickness of link 2   inches
t4=.003 !thickness of link 4  inches
theta30=0 !link 3 manufactured angle radians
rcouple=.20 !coupler length inches !
!-------------------------------Material---------------------------
--------------- E=30000000 !Modulus of
Elasticity lb/in^2 Pr=.3 !Poisson's
Ratio ----- sdc=1.2 !shear deflection
constant ----- !
```

```
!================================================================
=============== ! !                    OTHER PARAMETERS !
!================================================================
=============== ! t3=.25 !link 3 thickness,
stiffen inches r2=r1*s2 !length of link
2(PRBL) inches r3=r1*s3 !length of link
3(PRBL) inches r4=r1*s4 !length of link
4(PRBL) inches area2=t2*w !cross-sectional
area, link 2 inches^2 area3=t3*w !cross-sectional
area, link 3 inches^2 area4=t4*w !cross-sectional
area, link 4 inches^2 I2=w*t2**3/12 !Area moment
of inertia, link 2 inches^4 I3=w*t3**3/12 !Area
moment of inertia, link 3 inches^4
I4=w*t4**3/12 !Area moment of inertia, link
4 inches^4 ldiv=5 !Number of line
divisions ----- ldiv2=20 !Number of line
divisions ----- steps=180    !number of load
steps ----- *dim,xcouple,ARRAY,steps+1,1,1,!x
displacement of couple pt. inches
*dim,ycouple,ARRAY,steps+1,1,1,!y displacement of couple
pt. inches pi=ACOS(-1) !Definition of
pi radians
r5=((r3*COS(theta30*pi/180)-r1)**2+(r3*SIN(theta30*pi/180))**2)**0.5
x5=r3*COS(theta30*pi/180)-r1 y5=r3*sin(theta30*pi/180)

*IF,x5,EQ,0,AND,y5,GT,0,THEN !theta20 radians
theta20=ACOS((r4**2-r2**2-r5**2)/(2*r2*r5))+pi/2
*ELSEIF,x5,EQ,0,AND,y5,LT,0
theta20=ACOS((r4**2-r2**2-r5**2)/(2*r2*r5))-pi/2 *ELSEIF,x5,LT,0
theta20=ACOS((r4**2-r2**2-r5**2)/(2*r2*r5))-ATAN(y5/x5) *ELSE
theta20=ACOS((r4**2-r2**2-r5**2)/(2*r2*r5))+ATAN(y5/x5) *ENDIF

*IF,x5,EQ,0,AND,y5,GT,0,THEN !theta40 radians
theta40=ACOS((r4**2+r5**2-r2**2)/(2*r4*r5))+pi/2
*ELSEIF,x5,EQ,0,AND,y5,LT,0
theta40=ACOS((r4**2+r5**2-r2**2)/(2*r4*r5))-pi/2 *ELSEIF,x5,LT,0
theta40=ACOS((r4**2+r5**2-r2**2)/(2*r4*r5))-ATAN(y5/x5) *ELSE
theta40=ACOS((r4**2+r5**2-r2**2)/(2*r4*r5))+ATAN(y5/x5) *ENDIF

!================================================================
=============== ! ! SET UP BEAM ELEMENTS AND CONSTRAINTS
!
!================================================================
===============
```

```
ET,1,BEAM3 !2D Elastic Beam Element
R,2,area2,I2,t2,sdc,0,0,!Beam#2,AREA,Moment of
inertia,height,shearz,initial strain,added mass per unit length
R,3,area3,I3,t3,sdc,0,0,!Beam#3,AREA,Moment of
inertia,height,shearz,initial strain,added mass per unit length
R,4,area4,I4,t4,sdc,0,0,!Beam#4,AREA,Moment of
inertia,height,shearz,initial strain,added mass per unit length
UIMP,1,EX, , ,E,!Modulus of Elasticity UIMP,1,NUXY, ,
,Pr,!Poisson's Ratio UIMP,1,EMIS, ,
,1,!Emissivity=1 k,1,0,0 !Keypoints
#1-6 k,2,r2*cos(theta20)/.85,r2*sin(theta20)/.85
k,3,r1+r4*cos(theta40)/.85,r4*sin(theta40)/.85 k,4,r1,0
k,5,((((r2*cos(theta20)/.85)+(r1+r4*cos(theta40)/.85))/2)-rcouple*
sin(theta30)),(((r2*sin(theta20)/.85)+(r4*sin(theta40)/.85))/2)+
rcouple*cos(theta30)
k,6,(((r2*cos(theta20)/.85)+(r1+r4*cos(theta40)/.85))/2),(((r2*sin(
theta20)/.85)+(r4*sin(theta40)/.85))/2)
l,1,2 !Line from keypoint 1 to 2
l,2,6 !Line from keypoint 2 to 6
l,3,4 !Line from keypoint 3 to 4
l,6,5 !Line from keypoint 6 to 5
l,6,3 !Line from keypoint 6 to 3
esize,,ldiv2 !number of divisions per line
real,2 !Use real constant set 2
type,1 !Use element type "1", 2D Elastic Beam
mat,1 !Use element material properties "1"
lmesh,1 !Mesh lines 1-5 real,3 esize,,ldiv
lmesh,2 lmesh,5 lmesh,4 esize,,ldiv2 real,4 lmesh,3 FINISH
!=====================================================================
=============== ! ! SOLUTION !
!=====================================================================
=============== /SOLU NLGEOM,1 !Large deflection
analysis NROPT,AUTO, ,!Automatically choose
Newton-Raphson options LUMPM,0 !Element-dependent
default mass matrix EQSLV,FRONT,1e-08,0,!Solver: Front
direct, tolerance, multiplier SSTIF !Stress
stiffness "on" in nonlinear analysis
PSTRES !Prestress effects are calculated &
included TOFFST,0,!Temperature offset from absolute
0 to zero dk,1,ux,0 !Constrains keypoints 1 & 4 in x
and y dk,1,uy,0 dk,4,ux,0 dk,4,uy,0

!---------------------------Rotate the
Mechanism----------------------------------
```

```
dk,6,ux,-r2/40 !Translate to help prevent unwanted
buckling lswrite,1 !Write
dkdele,6,ux !Delete the constraint of translation
*DO,n,1,steps,1 !Rotate mechanism 360 deg. at kp 6 &
write dk,6,rotz,n*(2/steps)*Pi lswrite,n+1 *ENDDO
lssolve,1,steps+1 !Solves the written files /STAT,SOLU
FINISH

!=================================================================
=============== ! ! POST-PROCESSOR !
!=================================================================
=============== ! !------------------------Calculate & Output the
coupler curve---------------------- /POST1 *get,key5,kp,5,ATTR,NODE
*get,xcouple(1),NODE,key5,U,X *get,ycouple(1),NODE,key5,U,Y

*DO,n,2,steps+1 Set,n *get,xcouple(n),NODE,key5,U,X
*get,ycouple(n),NODE,key5,U,y *ENDDO

/output,couplecurve,txt !Outputs the couple curve points
for Excel *vwrite X Y *vwrite,xcouple(1),ycouple(1) %20e
%20e /output

!----------------------------Calculate the
Stresses--------------------------------

*DIM,smx,ARRAY,steps+1,1,1, *DIM,smn,ARRAY,steps+1,1,1, prrsol,
ksel,s,kp,,3 nslk,s *get,nkp3,node,0,num,max ksel,all nsel,all
*DO,n,1,steps+1,1 set,n ETABLE,smxi,NMIS,1 ETABLE,smxj,NMIS,3
esort,etab,smxi,0,0 *get,smx(n,1,1),sort,0,max eusort *ENDDO FINISH

!---------------Calculate the Torque in the "Spring" (Reaction
Moment)-------------- /POST26
*get,key6,kp,6,ATTR,NODE !retrieves the node value for
keypoint 6 nsol,2,key6,rot,z,rotz3 !for keypoint 6,
rotation in z is stored rforce,3,key6,m,z,mom3 !the total
reaction moment stored for kp 6
/output,stress,txt !Output the data to file "output"
*stat,smx,1,steps !Outputs the matrix smx to file
"output" !prvar,2,3,!Lists variables 2 and 3 w/
respect to time save /output /output,moment,txt !Output
the data to file "output" !*stat,smx,1,steps !Outputs the
matrix smx to file "output" prvar,2,3,!Lists
variables 2 and 3 w/ respect to time save /output FINISH

!=================================================================
```

```
================ ! ! END polypropylene_tristable.txt
!
!=================================================================
================
```

A.2 Tristable Mechanism With Coil Springs at the Joints

```
!================================================================
============== ! ! coil.txt !    ANSYS Batch File !
Created by Tyler Pendleton,  3 August 2005 !
!================================================================
============== ! FINISH /CLEAR /TITLE,  Stresses in beam of wire
tristable mechanism /PREP7 !
!================================================================
============== ! !                    INPUT PARAMETERS !
!================================================================
===============
!Variable Description Units
!--------------------------
!----------------------Geometry-------------------------------------
--------------- d=.0148 !diameter of
wire inches coilD=.1447 !mean diameter of
coil inches wraps=2 !integer # of wraps in
loops # wraps r1=.145 !length of link 1
inches s2=1.1 !scale of
r2:r1 ------ s3=1.1 !scale of
r3:r1 ------ s4=1.1 !scale of
r4:r1 ------ theta30=0 !theta
30 radians rcouple=.25 !coupler
length inches
!----------------------Material-------------------------------------
--------------- sdc=1.111 !shear deflection
constant ----- Ey=2.85E7 !Modulus of
Elasticity lb/in^2 Pr=.272 !Poisson's
Ratio -----
!================================================================
============== ! !--------------------Other
Parameters------------------------------------------ !
!================================================================
===============
!Variable Description Units
!--------------------------
pi=ACOS(-1) !Definition of pi radians
r2=r1*s2 !length of link 2(PRBL) inches
r3=r1*s3 !length of link 3(PRBL) inches
r4=r1*s4 !length of link 4(PRBL) inches
d2=.1 !increase stiffness of middle  inches
area=pi*d**2/4 !cross-sectional area    inches^2
area2=pi*d2**2/4 !cross-sectional area of
middle inches^2 I=pi*d**4/64         !Area moment of
```

```
inertia    inches^4 I2=pi*d2**4/64 !Area moment of
inertia, middle inches^4 type=1 !1=new,
0.85=old model ----- ldiv=1 !Number of
line divisions # div ldiv2=30 !Number of line
divisions # div steps=90    !number of load
steps # steps pieces=52.5 !total # of
divisions per loop # div kprotate=1
!2*wraps*pieces+7 !Where to rotate the mechanism ------
*dim,xcouple,ARRAY,steps+1,1,1,!x-coordinate of couple
point inches *dim,ycouple,ARRAY,steps+1,1,1,!y-coordinate
of couple point inches

r5=((r3*COS(theta30*pi/180)-r1)**2+(r3*SIN(theta30*pi/180))**2)**0.5
x5=r3*COS(theta30*pi/180)-r1 y5=r3*sin(theta30*pi/180)

*IF,x5,EQ,0,AND,y5,GT,0,THEN !theta20 radians
theta20=ACOS((r4**2-r2**2-r5**2)/(2*r2*r5))+pi/2
*ELSEIF,x5,EQ,0,AND,y5,LT,0
theta20=ACOS((r4**2-r2**2-r5**2)/(2*r2*r5))-pi/2 *ELSEIF,x5,LT,0
theta20=ACOS((r4**2-r2**2-r5**2)/(2*r2*r5))-ATAN(y5/x5) *ELSE
theta20=ACOS((r4**2-r2**2-r5**2)/(2*r2*r5))+ATAN(y5/x5) *ENDIF

*IF,x5,EQ,0,AND,y5,GT,0,THEN !theta40 radians
theta40=ACOS((r4**2+r5**2-r2**2)/(2*r4*r5))+pi/2
*ELSEIF,x5,EQ,0,AND,y5,LT,0
theta40=ACOS((r4**2+r5**2-r2**2)/(2*r4*r5))-pi/2 *ELSEIF,x5,LT,0
theta40=ACOS((r4**2+r5**2-r2**2)/(2*r4*r5))-ATAN(y5/x5) *ELSE
theta40=ACOS((r4**2+r5**2-r2**2)/(2*r4*r5))+ATAN(y5/x5) *ENDIF

r6=((r2/type)**2-(coilD/2)**2)**(1/2) !length of
r6 inches
r7=((r4/type)**2-(coilD/2)**2)**(1/2) !length of
r7 inches
thetaD1=ASIN(coilD/2/r2*type) !thetaD1 radians
thetaD2=ASIN(coilD/2/r4*type) !thetaD2 radians
theta6=ASIN(r6/r2*type) !theta6 radians
theta7=ASIN(r7/r4*type) !theta7 radians
phi1=pi+theta20-theta6 !phi1 radians
phi2=pi/2 !phi2 radians
totalangle1=wraps*2*pi+theta20-theta6+pi/2 !total angle, loop
1 radians totalangle2=wraps*2*pi+pi-theta40-theta7+pi/2 !total
angle, loop 2 radians
phip1=totalangle1/pieces/wraps !angle of one "piece" in loop
1 radians phip2=totalangle2/pieces/wraps !angle of one
"piece" in loop 2 radians !
```

```
!=================================================================
============== ! ! SET UP BEAM ELEMENTS AND CONSTRAINTS !
!=================================================================
============== ! ET,1,BEAM3 !2D Elastic Beam Element
R,2,area,I,d,sdc,0,0,!Beam#2,AREA,Moment of
inertia,height,shearz,initial strain,added mass per unit length
R,3,area2,I2,d2,sdc,0,0,!Beam#2,AREA,Moment of
inertia,height,shearz,initial strain,added mass per unit length
UIMP,1,EX, , ,Ey,!Modulus of Elasticity UIMP,1,NUXY, ,
,Pr,!Poisson's Ratio UIMP,1,EMIS, ,
,1,!Emissivity=1 k,1,0,0 !Keypoint #1
k,2,r2/type*cos(theta20),r2/type*sin(theta20) !Keypoint #2
k,3,r1+r4/type*cos(theta40),r4/type*sin(theta40) !Keypoint #3
k,4,r1,0 !Keypoint #4

*DO,n,5,wraps*pieces+5 !Keypoints for loop 1
k,n,r2/type*cos(theta20)+coilD/2*cos(phi1),r2/type*sin(theta20)+
coilD/2*sin(phi1) phi1=phi1-phip1 *ENDDO

!Keypoint for middle of crossmember
k,2*wraps*pieces+7,((r2/type*cos(theta20)+coilD/2*cos(phi1+phip1))+(
r1+r4/type*cos(theta40)+coilD/2*cos(phi2)))/2,((r2/type*sin(theta20)
+coilD/2*sin(phi1+phip1))+(r4/type*sin(theta40)+coilD/2*sin(phi2)))/
2 !Keypoint for couple point
k,2*wraps*pieces+8,((r2/type*cos(theta20)+coilD/2*cos(phi1+phip1))+(
r1+r4/type*cos(theta40)+coilD/2*cos(phi2)))/2,((r2/type*sin(theta20)
+coilD/2*sin(phi1+phip1))+(r4/type*sin(theta40)+coilD/2*sin(phi2)))/
2+rcouple*cos(theta30)

*DO,n,wraps*pieces+6,2*wraps*pieces+6 !Keypoints for loop 2
k,n,r1+r4/type*cos(theta40)+coilD/2*cos(phi2),r4/type*sin(theta40)+
coilD/2*sin(phi2) phi2=phi2-phip2 *ENDDO

l,1,5 !Lines for everything but the loops
l,2*wraps*pieces+6,4 l,wraps*pieces+5,2*wraps*pieces+7
l,2*wraps*pieces+7,wraps*pieces+6
l,2*wraps*pieces+7,2*wraps*pieces+8

*DO,n,5,wraps*pieces+4 !Lines for loop 1 l,n,n+1 *ENDDO

*DO,n,wraps*pieces+6,2*wraps*pieces+5 !Lines for loop 2 l,n,n+1
*ENDDO

esize,,ldiv2 !number of divisions per line
real,2 !Use real constant set 2
```

```
type,1 !Use element type "1", 2D elastic beam
mat,1 !Use material properties "1"
lmesh,1 !Mesh lines lmesh,2 real,3 esize,,ldiv2
lmesh,3 lmesh,4 lmesh,5 real,2 esize,,ldiv *DO,n,6,2*wraps*pieces+5
lmesh,n *ENDDO FINISH
!=====================================================================
=============== ! ! SOLUTION !
!=====================================================================
=============== /SOLU NLGEOM,1 !Large deflection
analysis NROPT,AUTO, ,!Automatically choose
Newton-Raphson options LUMPM,0 !Element-dependent
default mass matrix EQSLV,FRONT,1e-08,0,!Solver:Front
direct, tolerance, multiplier SSTIF !Stress
stiffness "on" in nonlinear analysis
PSTRES !Prestress effects calculated & included
TOFFST,0,!Temperature offset from absolute 0 to 0
dk,1,ux,0 !Constrains keypoints 1 & 4 in x and y
dk,1,uy,0 dk,4,ux,0 dk,4,uy,0

*DO,n,1,16 ksel,s,kp,,n+4 nslk,s *get,nkp1,node,0,num,max
ksel,s,kp,,n+49 nslk,s *get,nkp2,node,0,num,max ksel,s,kp,,n+94
nslk,s *get,nkp3,node,0,num,max ksel,all nsel,all
ce,next,0,nkp1,ux,1,nkp2,ux,-1,nkp3,ux,-1
!ce,next,0,nkp2,ux,1,nkp3,ux,-1
ce,next,0,nkp1,uy,1,nkp2,uy,-1,nkp3,uy,-1
!ce,next,0,nkp2,uy,1,nkp3,uy,-1 *ENDDO

*DO,n,17,61 ksel,s,kp,,n+4 nslk,s *get,nkp1,node,0,num,max
ksel,s,kp,,n+49 nslk,s *get,nkp2,node,0,num,max ksel,all nsel,all
ce,next,0,nkp1,ux,1,nkp2,ux,-1 ce,next,0,nkp1,uy,1,nkp2,uy,-1 *ENDDO

*DO,n,110,125 ksel,s,kp,,n nslk,s *get,nkp1,node,0,num,max
ksel,s,kp,,n+45 nslk,s *get,nkp2,node,0,num,max ksel,s,kp,,n+90
nslk,s *get,nkp3,node,0,num,max ksel,all nsel,all
ce,next,0,nkp1,ux,1,nkp2,ux,-1,nkp3,ux,-1
!ce,next,0,nkp2,ux,1,nkp3,ux,-1
ce,next,0,nkp1,uy,1,nkp2,uy,-1,nkp3,uy,-1
!ce,next,0,nkp2,uy,1,nkp3,uy,-1 *ENDDO

*DO,n,126,167 ksel,s,kp,,n nslk,s *get,nkp1,node,0,num,max
ksel,s,kp,,n+45 nslk,s *get,nkp2,node,0,num,max ksel,all nsel,all
ce,next,0,nkp1,ux,1,nkp2,ux,-1 ce,next,0,nkp1,uy,1,nkp2,uy,-1 *ENDDO
```

```
!-----------------------Rotate the
Mechanism--------------------------------------
!dk,2*wraps*pieces+7,ux,-r2/20 !Translate to help prevent
unwanted buckling !lswrite,1 !Write the data
!dkdele,2*wraps*pieces+7,ux !Delete the constraint of
translation

*DO,n,1,steps,1 !Rotate 360 degrees at kp "kprotate"
& write dk,kprotate,rotz,n*(2/steps)*Pi lswrite,n *ENDDO
lssolve,1,steps !Solves the written files /STAT,SOLU
FINISH
!=====================================================================
=============== ! ! POST-PROCESSOR !
!=====================================================================
=============== !-----------------------Calculate & Output the
coupler curve----------------------- /POST1
*get,key100,kp,kprotate,ATTR,NODE !Retrieves nodal value for kp
"kprotate" *get,xcouple(1),NODE,key100,U,X !Retrieves x-value
for position 1 *get,ycouple(1),NODE,key100,U,Y !Retrieves
y-value for position 1

*DO,n,2,steps+1 !Retrieves x&y values for remaining
posions Set,n *get,xcouple(n),NODE,key100,U,X
*get,ycouple(n),NODE,key100,U,y *ENDDO

/output,couplecurve,txt !Outputs the couple curve points
for Excel *vwrite X Y *vwrite,xcouple(1),ycouple(1) %20e
%20e /output

!-----------------------Calculate the
Stresses--------------------------------------
*DIM,smx,ARRAY,steps+1,1,1, *DIM,smn,ARRAY,steps+1,1,1, prrsol,
ksel,s,kp,,3 nslk,s *get,nkp3,node,0,num,max ksel,all nsel,all
*DO,n,1,steps+1,1 set,n ETABLE,smxi,NMIS,1 ETABLE,smxj,NMIS,3
esort,etab,smxi,0,0 *get,smx(n,1,1),sort,0,max eusort *ENDDO FINISH

!------------------Calculate the Reaction Moment at the Rotational
Kepoint---------- /POST26 nsol,2,key100,rot,z,rotz !for kp
key100, z-rotation stored (rotz)
rforce,3,key100,m,z,mom !for kp key100, store reaction
moment (mom) !rforce,3,key100,f,x,force !for kp key100,
store reaction moment (mom) /output,output,txt !Output
the data to file "output" !*stat,smx,1,steps !Output the
matrix smx to file "output" prvar,2,3,!List
```

```
variables 2 and 3 w/ respect to time save /output FINISH
!=====================================================================
=============== ! ! END coil.txt !
!=====================================================================
===============
```

A.3 Tristable Mechanism with Torsion Bars

```
!================================================================
============== ! ! torsionbar.txt !    ANSYS Batch File !
Created by Tyler Pendleton,  10 April 2006 ! Created to
analyze suspected higher stress due to bend angle ! Added kp
halfway between bends 3,4 and changed the Pr and E, 11 July !
!================================================================
============== ! FINISH /CLEAR /TITLE,  Stresses in beam of wire
tristable mechanism /PREP7 !
!================================================================
============== ! !                    INPUT PARAMETERS !
!================================================================
==============
!Variable Description Units
!--------------------------
!----------------------Geometry-----------------------------------
--------------- r=0.08 !radius of
bends inches width=0.8857 !out of plane width
in torsion  inches width2=0.25 !out of plane
width, pin joint inches d=0.0286 !diameter of
wire inches r1=.0975 !length of link 1
inches s2=2.8 !scale of
r2:r1 ------ s3=1.67 !scale of
r3:r1 ------ s4=2.8 !scale of
r4:r1 ------ theta30=0 !theta
30 radians rcouple=.25 !coupler
length inches bendangle=20 !bend
angle degrees
!-----------------------Material-----------------------------------
--------------- sdc=(10/9) !shear deflection
constant ----- shearz=sdc !sdc on the z direction
sheary=sdc !sdc in the y direction Ex=2.85E7
Ey=2.85E7 !Modulus of Elasticity lb/in^2
Pr=.272 !Poisson's Ratio -----
!================================================================
============== ! !--------------------Other
Parameters------------------------------------------- !
!================================================================
==============
!Variable Description Units
!--------------------------
pi=ACOS(-1) !Definition of pi radians
bendangle=bendangle*pi/180 !bendangle in
radians radians r2=r1*s2 !length of link
```

```
2(PRBL) inches r3=r1*s3 !length of link
3(PRBL) inches r4=r1*s4 !length of link
4(PRBL) inches d2=d !increase stiffness of
middle  inches area=pi*d**2/4 !cross-sectional
area    inches^2 area2=pi*d2**2/4 !cross-sectional
area of middle inches^2 IZZ=(pi/64)*d**4 !Area moment
of inertia    inches^4 IYY=(pi/64)*d**4 !Area moment
of inertia    inches^4 IXX=(pi/32)*d**4 !Polar moment
of inertia    inches^4 OD=d OD2=d2 TKWALL=d/2 TKWALL2=d2/2 tkz=d
tky=d theta=0 istrn=0 spin=0 addmas=0
I2=pi*d2**4/64 !Area moment of inertia,
middle inches^4 type=1 !1=new, 0.85=old
model ----- ldiv=50 !Number of line
divisions # div ldiv2=50 ldiv3=1 !Number of line
divisions # div steps=90    !number of load
steps # steps pieces=30 !total # of divisions
per loop # div kprotate=6*ldiv+9 !Where to rotate the
mechanism ------ kprotate2=4*ldiv+4 !Where to rotate
the mechanism  ------
*dim,xcouple,ARRAY,steps,1,1,!x-coordinate of couple
point inches *dim,ycouple,ARRAY,steps,1,1,!y-coordinate
of couple point inches

r5=((r3*COS(theta30*pi/180)-r1)**2+(r3*SIN(theta30*pi/180))**2)**0.5
x5=r3*COS(theta30*pi/180)-r1 y5=r3*sin(theta30*pi/180)

*IF,x5,EQ,0,AND,y5,GT,0,THEN !theta20 radians
theta20=ACOS((r4**2-r2**2-r5**2)/(2*r2*r5))+pi/2
*ELSEIF,x5,EQ,0,AND,y5,LT,0
theta20=ACOS((r4**2-r2**2-r5**2)/(2*r2*r5))-pi/2 *ELSEIF,x5,LT,0
theta20=ACOS((r4**2-r2**2-r5**2)/(2*r2*r5))-ATAN(y5/x5) *ELSE
theta20=ACOS((r4**2-r2**2-r5**2)/(2*r2*r5))+ATAN(y5/x5) *ENDIF

*IF,x5,EQ,0,AND,y5,GT,0,THEN !theta40 radians
theta40=ACOS((r4**2+r5**2-r2**2)/(2*r4*r5))+pi/2
*ELSEIF,x5,EQ,0,AND,y5,LT,0
theta40=ACOS((r4**2+r5**2-r2**2)/(2*r4*r5))-pi/2 *ELSEIF,x5,LT,0
theta40=ACOS((r4**2+r5**2-r2**2)/(2*r4*r5))-ATAN(y5/x5) *ELSE
theta40=ACOS((r4**2+r5**2-r2**2)/(2*r4*r5))+ATAN(y5/x5) *ENDIF

!
!================================================================
============== ! ! SET UP BEAM ELEMENTS AND CONSTRAINTS !
!================================================================
============== ! ET,1,PIPE16 !3D Elastic Beam
```

```
Element R,1,OD,TKWALL !Beam #1, Outer diameter, wall
thickness R,2,OD2,TKWALL2 !Beam #2, Outer diameter,
wall thickness UIMP,1,EX, , ,Ey,!Modulus of Elasticity
UIMP,1,NUXY, , ,Pr,!Poisson's Ratio UIMP,1,EMIS, ,
,1,!Emissivity=1
k,1,0,0,-width2 !Keypoint #1

theta=0 !Bend #1 *DO,n,2,ldiv+2
k,n,-r*(1-cos(theta))*sin(theta20-pi/2),r*(1-cos(theta))*cos(theta20
-pi/2),r*sin(theta) theta=theta+(Pi/2-bendangle)/ldiv *ENDDO

*DO,n,2,ldiv+1 !Lines for bend #1 l,n,n+1 *ENDDO

theta=-bendangle !Bend #2 *DO,n,ldiv+3,2*ldiv+3
k,n,-(r2-r+r*sin(theta))*(sin(theta20-pi/2)),(r2-r+r*sin(theta))*cos
(theta20-pi/2),(r2-2*r)*tan(bendangle)+r*cos(theta)
theta=theta+(Pi/2+bendangle)/ldiv *ENDDO

*Do,n,ldiv+3,2*ldiv+2 !Lines for bend #2 l,n,n+1 *Enddo

r0=r theta=0 !Bend #3, 90 degree bend
*DO,n,2*ldiv+4,3*ldiv+4
k,n,r2*cos(theta20)+(r0-r0*cos(theta))*cos(theta30),r2*sin(theta20)+
(r0-r0*cos(theta))*sin(theta30),(r2-2*r)*tan(bendangle)-(width-r0+r0
*sin(theta)) theta=theta+Pi/ldiv/2 *ENDDO

*Do,n,2*ldiv+4,3*ldiv+3 !Lines for bend #3 l,n,n+1 *Enddo

theta=0 !Bend #4, 90 degree bend
*DO,n,3*ldiv+5,4*ldiv+5
k,n,r1+r4*cos(theta40)-(r0-r0*cos(theta))*cos(theta30),r4*sin(
theta40)-(r0-r0*cos(theta))*sin(theta30),(r2-2*r)*tan(bendangle)-(
width-r0+r0*sin(theta)) theta=theta+Pi/ldiv/2 *ENDDO

*Do,n,3*ldiv+5,4*ldiv+4 !Lines for bend #4 l,n,n+1 *Enddo

theta=-bendangle !Bend #5 *DO,n,4*ldiv+6,5*ldiv+6
k,n,r1+(r4-r+r*sin(theta))*sin(pi/2-theta40),(r4-r+r*sin(theta))*cos
(pi/2-theta40),(r2-2*r)*tan(bendangle)+r*cos(theta)
theta=theta+(Pi/2+bendangle)/ldiv *ENDDO
*Do,n,4*ldiv+6,5*ldiv+5 !Lines for bend #5 l,n,n+1 *Enddo


theta=0 !Bend #6 *DO,n,5*ldiv+7,6*ldiv+7
k,n,r1+r*(1-cos(theta))*sin(pi/2-theta40),r*(1-cos(theta))*cos(pi/2-
```

```
theta40),r*sin(theta) theta=theta+(Pi/2-bendangle)/ldiv *ENDDO

*Do,n,5*ldiv+7,6*ldiv+6 !Lines for bend #6 l,n,n+1 *Enddo

k,6*ldiv+8,r1,0,-width2 !Last Keypoint theta=pi/2
k,6*ldiv+9,((r2*cos(theta20)+(r0-r0*cos(theta))*cos(theta30))+(r1+r4
*cos(theta40)-(r0-r0*cos(theta))*cos(theta30)))/2,r2*sin(theta20)+(
r0-r0*cos(theta))*sin(theta30),(r2-2*r)*tan(bendangle)-(width-r0+r0*
sin(theta))


l,1,2 !First Line l,ldiv+2,ldiv+3 !Line
between bends 1 and 2 l,2*ldiv+3,2*ldiv+4 !Line between bends
2 and 3 l,3*ldiv+4,6*ldiv+9 !Line between bends 3 and 4
l,6*ldiv+9,4*ldiv+5 !Line between bends 3 and 4
l,3*ldiv+5,5*ldiv+6 !Line between bends 4 and 5
l,4*ldiv+6,6*ldiv+7 !Line between bends 5 and 6
l,5*ldiv+7,6*ldiv+8 !Last line



esize,,1 !number of divisions per line
real,1 !Use real constant set 2
type,1 !Use element type "1", 3D elastic beam
mat,1 !Use material properties "1"

*DO,n,1,6*ldiv lmesh,n *ENDDO

esize,,ldiv2 *DO,n,6*ldiv+1,6*ldiv+3 lmesh,n *ENDDO

esize,,5 real,2 lmesh,6*ldiv+4 lmesh,6*ldiv+5

esize,,ldiv2 real,1 *DO,n,6*ldiv+6,6*ldiv+8 lmesh,n *ENDDO FINISH
!=====================================================================
=============== ! ! SOLUTION !
!=====================================================================
=============== /SOLU NLGEOM,1 !Large deflection
analysis NROPT,AUTO, ,!Automatically choose
Newton-Raphson options LUMPM,0 !Element-dependent
default mass matrix EQSLV,FRONT,1e-08,0,!Solver:Front
direct, tolerance, multiplier SSTIF !Stress
stiffness "on" in nonlinear analysis
PSTRES !Prestress effects calculated & included
TOFFST,0,!Temperature offset from absolute 0 to 0
dk,1,ux,0 !Constrains first keypoint in xyz dk,1,uy,0
```

```
dk,1,uz,0 dk,2,ux,0 !Constrains second keypoint in xy
dk,2,uy,0 dk,5*ldiv+7,ux,0 !Constrains second to last
keypoint in xy dk,5*ldiv+7,uy,0
dk,6*ldiv+8,ux,0 !constrains last keypoint in xyz
dk,6*ldiv+8,uy,0 dk,6*ldiv+8,uz,0
dk,3*ldiv+4,uz,0 !Constrains kps on line between bends
3,4 dk,4*ldiv+5,uz,0 ksel,s,kp,,2*ldiv+3 nslk,s
*get,nkp2,node,0,num,max ksel,s,kp,,5*ldiv+6 nslk,s
*get,nkp3,node,0,num,max ksel,s,kp,,2*ldiv+4 nslk,s
*get,nkp5,node,0,num,max ksel,s,kp,,3*ldiv+5 nslk,s
*get,nkp6,node,0,num,max ksel,all nsel,all
ce,1,0,nkp2,ux,1,nkp5,ux,-1    !Constrains the portion in the
slot ce,2,0,nkp3,ux,1,nkp6,ux,-1 !ce,1,-0.0032,nkp2,ux,1,nkp5,ux,-1
!Use for simulating slot clearance !ce,2,0.0032,nkp3,ux,1,nkp6,ux,-1
ce,3,0,nkp2,uy,1,nkp5,uy,-1 ce,4,0,nkp3,uy,1,nkp6,uy,-1
ce,5,0,nkp2,rotx,1,nkp5,rotx,-1 ce,6,0,nkp2,roty,1,nkp5,roty,-1
ce,7,0,nkp3,rotx,1,nkp6,rotx,-1 ce,8,0,nkp3,roty,1,nkp6,roty,-1

!-----------------------Rotate the
Mechanism--------------------------------------
!dk,4*ldiv+13,ux,-r1/20 !lswrite,n !dkdele,4*ldiv+13,ux a=0 !Use if
above is commented out *DO,n,1+a,steps+a,1 !Rotate
360 degrees at kp "kprotate" & write
!dk,4*ldiv+13,rotz,n*(1/steps)*Pi dk,kprotate,rotz,n*(1/steps)*Pi
! dk,kprotate2,rotz,n*(1/steps)*Pi lswrite,n *ENDDO
lssolve,1,steps+a !Solves the written files /STAT,SOLU
FINISH
!=====================================================================
================ ! ! POST-PROCESSOR !
!=====================================================================
================ !----------------------Calculate & Output the
coupler curve----------------------- /POST1
!*get,key100,kp,4*ldiv+13,ATTR,NODE !Retrieves nodal value for kp
"kprotate" *get,key100,kp,kprotate,ATTR,NODE !Retrieves nodal
value for kp "kprotate"

!*get,xcouple(1),NODE,key100,U,X !Retrieves x-value for
position 1 !*get,ycouple(1),NODE,key100,U,Y !Retrieves
y-value for position 1

!*DO,n,2,steps+1 !Retrieves x&y values for remaining
posions ! Set,n ! *get,xcouple(n),NODE,key100,U,X
! *get,ycouple(n),NODE,key100,U,y !*ENDDO

!/output,couplecurve,txt !Outputs the couple curve points
```

```
for Excel !*vwrite ! X Y
!*vwrite,xcouple(1),ycouple(1) !%20e %20e !/output

!----------------------Calculate the
Stresses-------------------------------------
*DIM,torsion,ARRAY,steps+a,1,1, *DIM,bending,ARRAY,steps+a,1,1,
*DIM,bending2,ARRAY,152,steps+a,1 *DIM,vonmis,ARRAY,steps+a,1,1,
prrsol, ksel,s,kp,,3 nslk,s *get,nkp3,node,0,num,max !ksel,all
nsel,none nsel,s,node,,1,100 nsel,a,node,,357,405 esln,all
*DO,n,1,steps+a,1 set,n ETABLE,vonmises,nmisc,89 ETABLE,sshear,ls,4
ETABLE,sbend,nmisc,92 ETABLE,s1,nmisc,86 ETABLE,smxi,NMIS,1
ETABLE,smxj,NMIS,3 esort,etab,sshear,0,0
*get,torsion(n,1,1),sort,0,max esort,etab,sbend,0,0
*get,bending(n,1,1),sort,0,max esort,etab,vonmises,0,0
*get,vonmis(n,1,1),sort,0,max eusort *ENDDO FINISH

!------------------Calculate the Reaction Moment at the Rotational
Kepoint---------- /POST26 nsol,2,key100,rot,z,rotz !for kp
key100, z-rotation stored (rotz)
rforce,3,key100,m,z,mom !for kp key100, store reaction
moment (mom) /output,moment,txt prvar,2,3, save /output
/output,shear,txt !File for the maximum shear stress
*stat,torsion,1,steps+a !Output the array "torsion" to
file "shear" save /output /output,bend,txt !File for the
maximum bending stress *stat,bending,1,steps+a !Output
the array "bending" to file "bend" save /output
/output,vonmises,txt !File for the maxiumum von mises
stress *stat,vonmis,1,steps+a !Output the array "von
mises" to file "output" save /output FINISH
!=================================================================
============== ! ! END torsionbar.txt !
!=================================================================
===============
```

Appendix B

Timeline of Prototypes

This appendix is a history of the development of a prototype hinge.

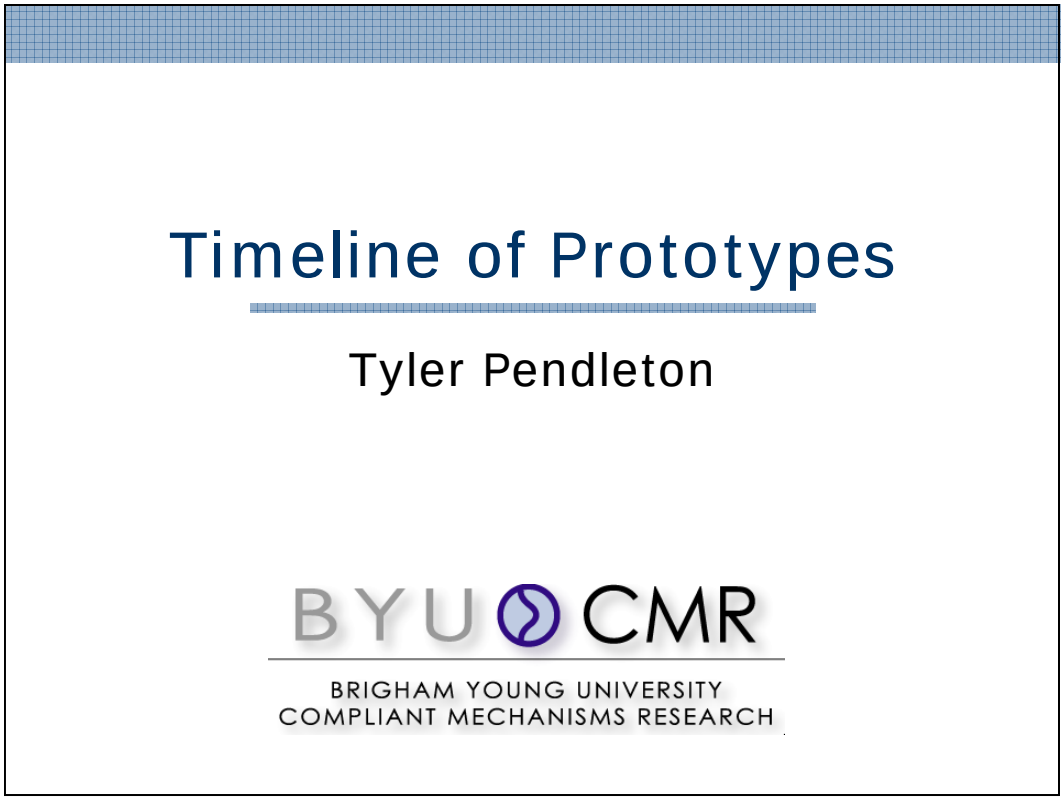

Original Tristable Mechanism

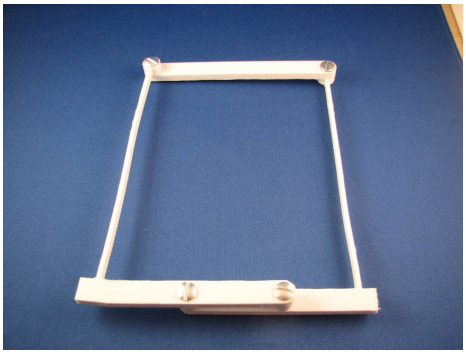

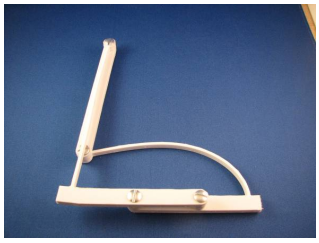

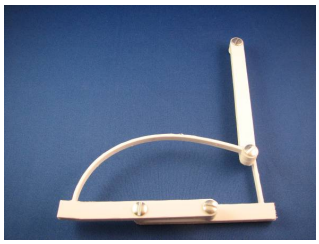

Date: ~2002

BYU CMR

First Hinge

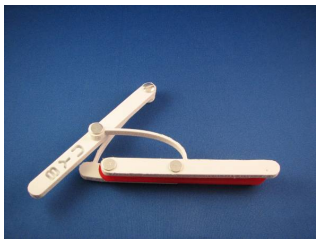

Date: 5/18/05

BYU CMR

1st "Fully compliant" tristable mechanism

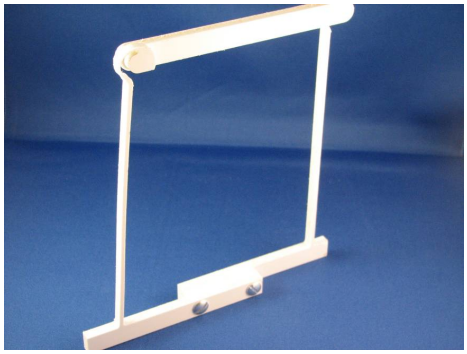

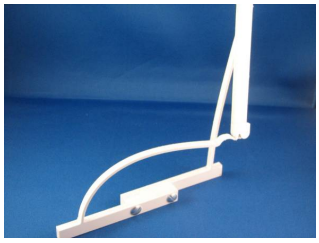

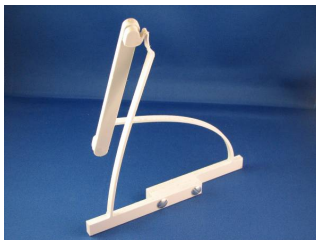

Date: 6/13/05

BYU CMR

First Miniaturization

Date: 6/21/05

BYU CMR

ABS Tristable Mechanism

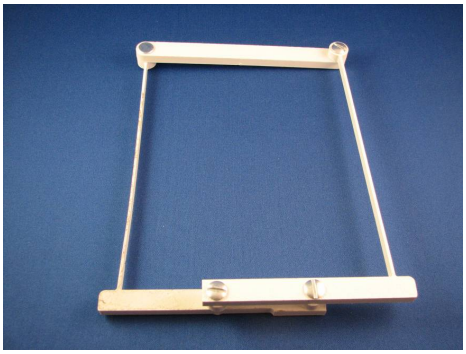

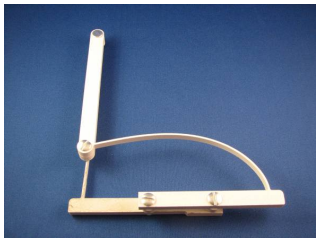

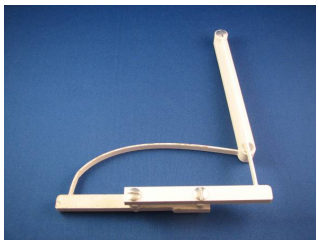

Date: 7/6/05

BYU CMR

1st Wireform Tristable Mechanism

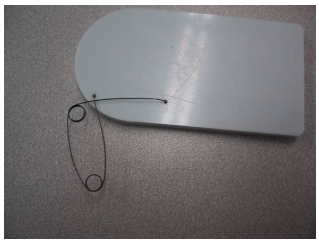

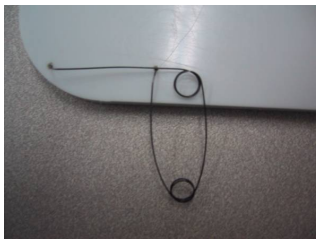

Date: 7/11/05

BYU CMR

Wireform implemented into "twist" hinge

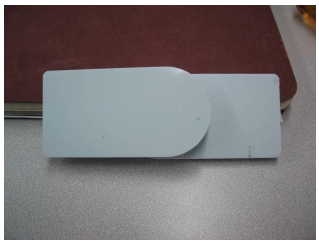

Date: 7/12/05

BYU CMR

Rev B on "twist" hinge

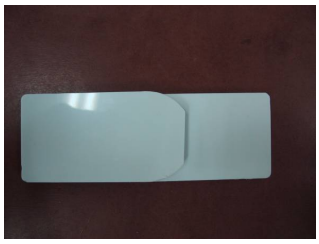

Date: 7/15/05

BYU CMR

Miniaturized wireform mechanism

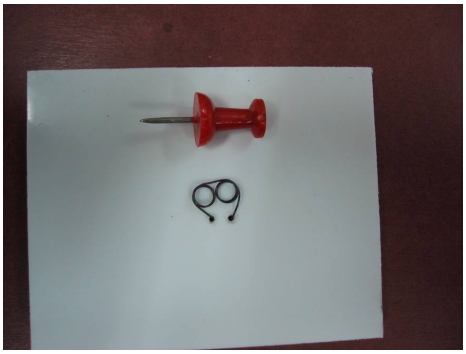

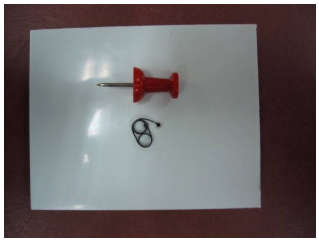

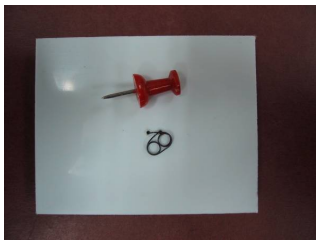

Date: 7/21/05

BYU CMR

Demonstration of PRBM

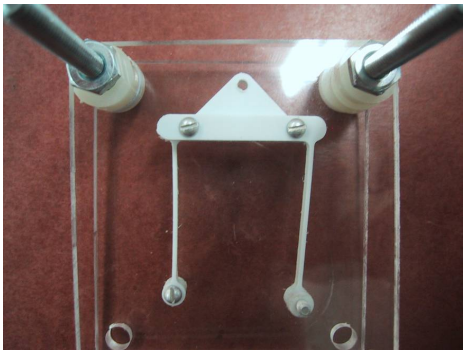

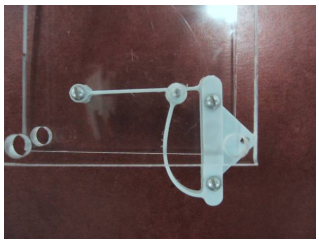

Date: 7/26/05

BYU CMR

Implemented into hinge

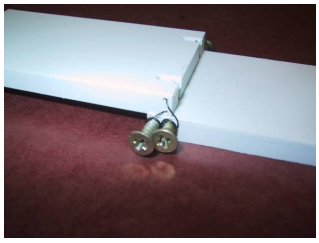

Date: 8/18/05

BYU CMR

Sheet Metal Tristable Mechanism

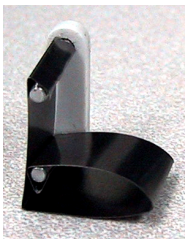

Date: 8/20/05

BYU CMR

Flexible segments tristable hinge

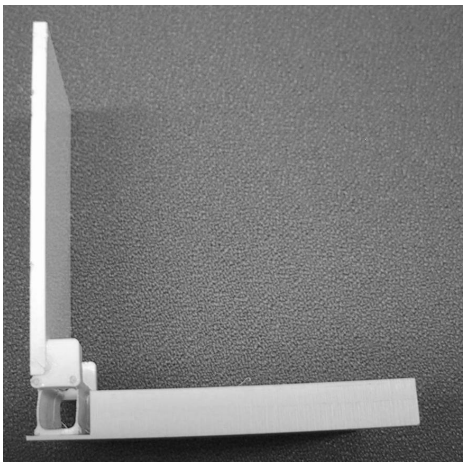

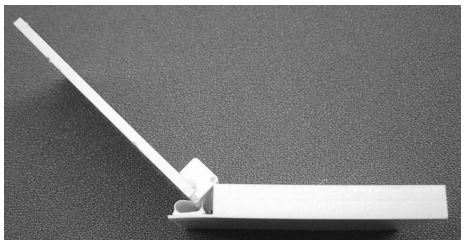

Date: 8/26/05

BYU CMR

Rev B Torsion Bar Tristable

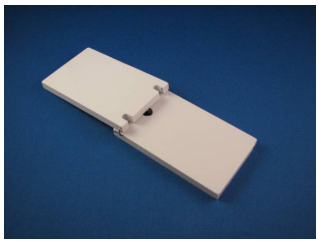

Date: 9/8/05

BYU CMR

Rev C Torsion Bar Tristable

Date: 9/13/05

BYU CMR

Fully Compliant Tristable Mechanism: Small-length flexural pivots & living hinges

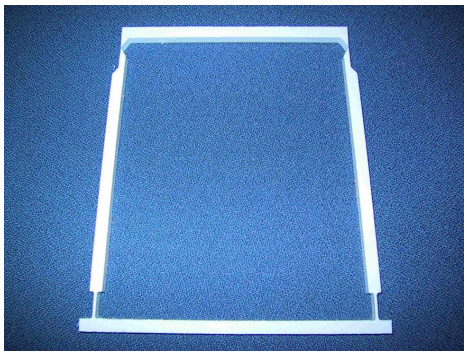

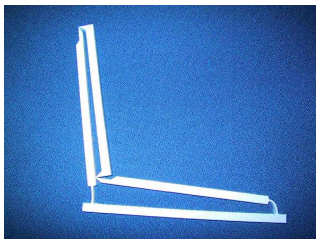

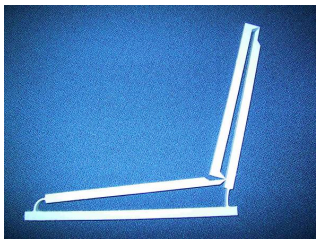

Date: 9/13/05

BYU CMR

Fully compliant tristable mechanism: Flexible segments & living hinges

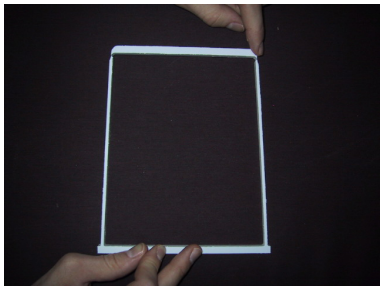

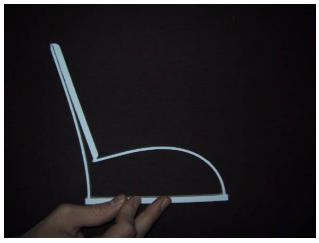

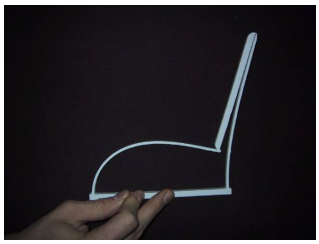

Date: 10/4/05

BYU CMR

Final Demonstrator

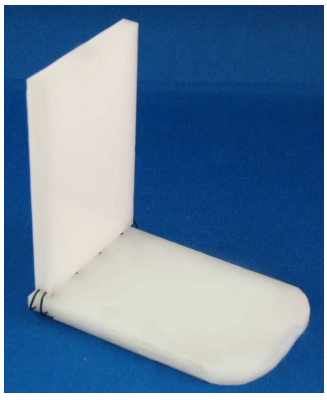

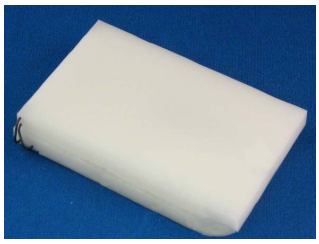

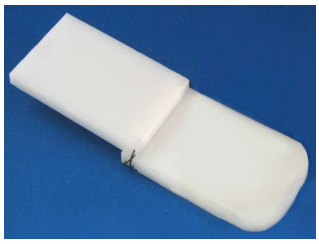

Date: 1/4/06

BYU CMR

Bibliography

[1] A. G. Erdman and G. N. Sandor, *Mechanism Design: Analysis and Synthesis*, 3rd ed. Prentice Hall, Upper Saddle River, NJ, 1997, vol. 1.

[2] J. E. Shigley and J. J. Uicker, *Theory of Machines and Mechanisms*, 2nd ed. McGraw-Hill, New York, 1995.

[3] L. L. Howell, *Compliant Mechanisms*. John Wiley & Sons, 2001.

[4] S. P. Timoshenko, *Theory of Elastic Stability*, 2nd ed. McGraw-Hill, New York, 1961.

[5] S. P. Timoshenko and D. H. Young, *Engineering Mechanics*, 3rd ed. McGraw-Hill, New York, 1951.

[6] G. J. Simitses, *An Introduction to the Elastic Stability of Structures*. Prentice Hall, Upper Saddle River, NJ, 1976.

[7] H. Leipholz, *Stability Theory*. Academic Press, New York and London, 1970.

[8] C. R. Mortensen, B. L. Weight, L. L. Howell, and S. P. Magleby, "Compliant mechanism prototyping," in *Proc. ASME 2000 Design Engineering Technical Conferences*, 2000, paper DETC2000/MECH-14204.

[9] L. Euler, *Methodus Inveniendi Leneas Curvas Maximi Minimive Peoprietate Gavdentes*. Lausanne and Beneva (Latin), 1744, (For English, see Isis vol. 20, Bruges, Belgium, November 1933.).

[10] K. E. Bisshop and D. C. Drucker, "Large deflection of cantilever beams," *Quarterly of Applied Mathematics*, vol. 3, no. 3, pp. 272–275, 1945.

[11] L. L. Howell and A. Midha, "A method for the design of compliant mechanisms with small-length flexural pivots," *ASME Journal of Mechanical Design*, vol. 116, no. 1, pp. 280–290, 1994.

[12] F. Grashof, *Theroetische Mashinenlehre*. Leipzig, 1883.

[13] B. Paul, "A reassessment of grashof's criterion," *ASME Journal of Mechanical Design*, vol. 101, pp. 515–518, 1979.

[14] C. R. Barker, "A complete classification of planar four-bar linkages," *Mechanism and Machine Theory*, vol. 20, no. 6, pp. 535–554, 1985.

[15] P. G. Opdahl, B. D. Jensen, and L. L. Howell, "An investigation into compliant bistable mechanisms," in *Proc. 1998 ASME Design Engineering Technical Conferences*, 1998, paper DETC98/MECH-5914.

[16] B. D. Jensen, M. B. Parkinson, K. Kurabayashi, L. L. Howell, and M. S. Baker, "Design optimization of a fully-compliant bistable micro-mechanism," in *Microelectromechanical Systems (MEMS)*. 2001 ASME Int. Mechanical Engineering Congress and Exposition, 2001, paper IMECE2001/MEMS-23852.

[17] M. T. A. Saif, "On a tunable bistable MEMS—theory and experiment," *J. Microelectromech. Syst.*, vol. 9, no. 2, pp. 157–170, June 2000.

[18] J. Qiu, J. H. Lang, and A. H. Slocum, "A curved-beam bistable mechanism," *J. Microelectromech. Syst.*, vol. 13, no. 2, pp. 137–146, April 2004.

[19] B. D. Jensen and L. L. Howell, "Identification of compliant pseudo-rigid-body mechanism configurations resulting in bistable behavior," *J. Mechanical Design*, vol. 125, no. 4, pp. 701–708, 2003.

[20] ——, "Bistable configurations of compliant mechanisms modeled using four links and translational joints," *J. Mechanical Design*, vol. 126, no. 4, pp. 657–666, 2004.

[21] M. Ohsaki and S. Nishiwaki, "Shape design of pin-jointed multistable compliant mechanisms using snapthrough behavior," *Struct. Multidisc. Optim.*, vol. 30, pp. 327–334, 2005.

[22] H.-J. Su and J. M. McCarthy, "Synthesis of compliant mechanisms with specified equilibrium positions," in *ASME 2005 Int. Des. Eng. Tech. Conf.*, no. DETC2005-85085, 2005.

[23] C. W. King, M. I. Campbell, J. J. Beaman, and S. V. Sreenivasan, "Synthesis of multistable equilibrium linkage systems using and optimization approach," *Struct. Multidisc. Optim.*, vol. 29, pp. 477–487, 2005.

[24] M. Hafez, M. D. Lichter, and S. Dubowsky, "Optimized binary modular reconfigurable robotic devices," *IEEE/ASME Trans. Mechatronics*, vol. 8, no. 1, pp. 18–25, March 2003.

[25] A. Herring, S. P. Magleby, L. H. Howell, and R. H. Todd, "High production manufacturing considerations for metallic compliant mechanisms with long thin beams," in *Proc. ASME 2001 Design Engineering Technical Conferences*, 2001, paper DETC2001/DFM-00001.

[26] P. Soroushian, H. Chowdhury, and A. Nossoni, "Design and experimental verification of pseudoelastic-based constant-force springs," *Journal Of Intelligent Material Systems And Structures*, vol. 14, no. 8, pp. 475–481, 2003.

[27] C. Vehar, S. Kota, and R. Dennis, "Closed-loop tape springs as fully compliant mechanisms - preliminary investigations," in *Proc. ASME 2004 Design Engineering Technical Conferences*, 2004, paper DETC2004-57403.

[28] J. Parise, L. L. Howell, and S. P. Magleby, "Ortho-planar linear-motion springs," *Mechanism and Machine Theory*, vol. 36, no. 11-12, pp. 1281–1299, 2001.

[29] N. O. Rasmussen, "Behavior of compliant orth-planar springs under complex loads," Master's thesis, Brigham Young University, 2005.

[30] A. Robison, "Modeling and validation of tension element based mechanisms for golf ball-club impact," Master's thesis, Brigham Young University, 2006.

[31] S. F. Miller, C. Kao, A. J. Shih, and J. Qu, "Investigation of wire electrical discharge machining of thin cross-sections and compliant mechanisms," *International Journal of Machine Tools & Manufacture*, vol. 45, no. 15, pp. 1717–1725, 2005.

[32] J. R. Cannon and L. L. Howell, "A compliant contact-aided revolute joint," *Mechanism & Machine Theory*, vol. 40, no. 11, pp. 1273–1293, 2005.

[33] N. B. Crane, L. L. Howell, B. L. Weight, and S. P. Magleby, "Compliant floating-opposing-arm (foa) centrifugal clutch," *Journal of Mechanical Design*, vol. 126, no. 1, pp. 169–177, 2004.

[34] J. E. Shigley, C. R. Mischke, and R. G. Budynas, *Mechanical Engineering Design*, 7th ed. McGraw-Hill, 2004.

[35] Personal communication with Ron Mongeon, Spring Works Utah, January 2006.

[36] J. M. Gere, *Mechanics of Materials*, 5th ed. Brooks/Cole, 2001.